MECHANICAL ENGINEERING SCIENCE

ISSN:2661-4448(online)
2661-443X(print)
Volume 5 No.1 2023

VISER
www.viserdata.com

COMPANY INTRODUCTION

Viser Technology Pte. Ltd. was founded in Singapore with branch offices in both Hebei and Chongqing, China. Viser focuses on publishing scientific and technological journals and books that promote the exchange of scientific and technological findings among the research community and around the globe. Despite being a young company, Viser is actively connecting with well-known universities, research institutes, and indexation database, and has already established a stable collaborative relationship with them. We also have a group of experienced editors and publishing experts who are dedicated to publishing high-quality journal and book contents. We offer the scholars various academic journals covering a variety of subjects and we are committed to reducing the hassles of scholarly publishing. To achieve this goal, we provide scholars with an all-in-one platform that offers solutions to every publishing process that a scholar needs to go through in order to show their latest finding to the world.

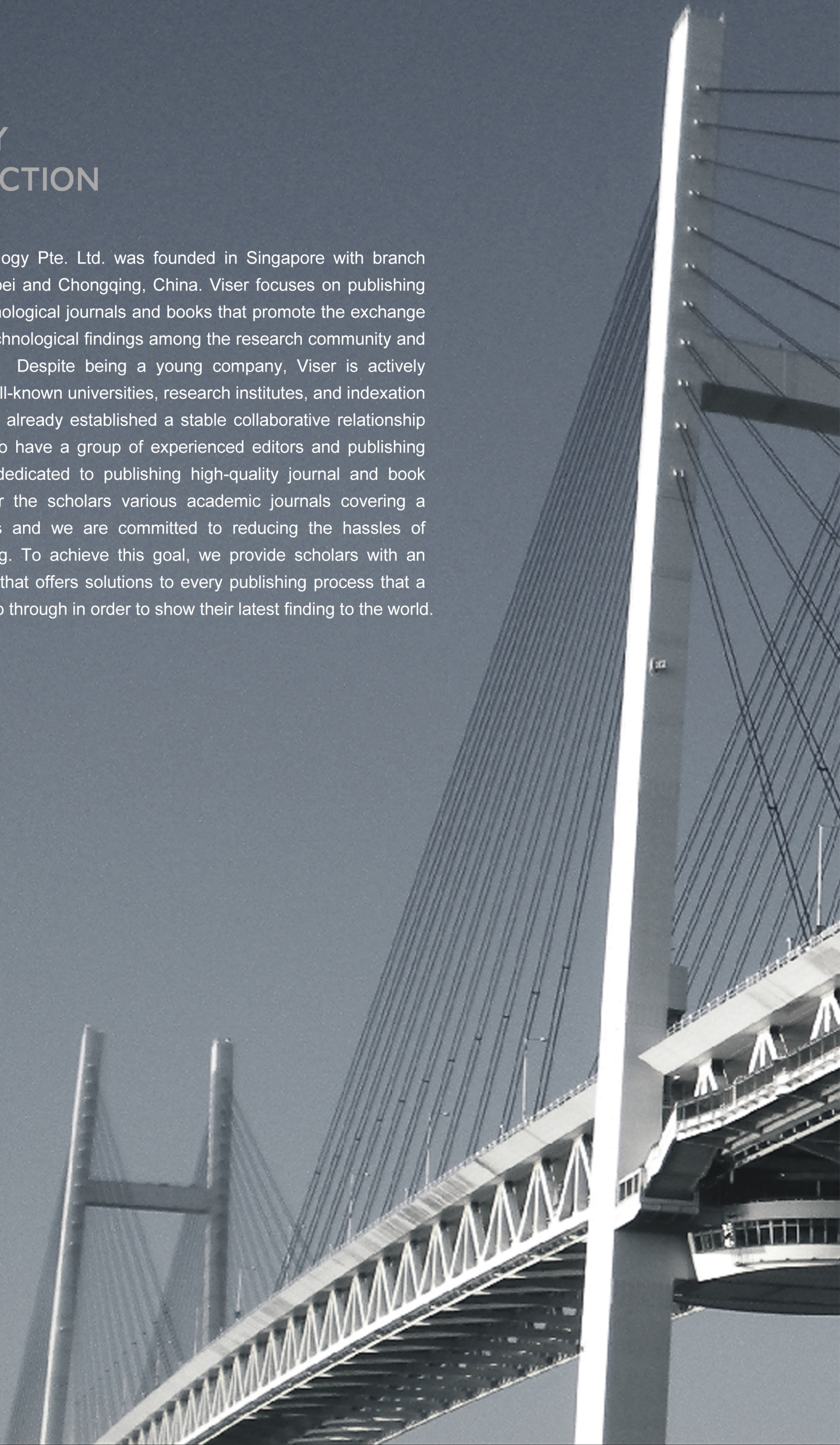

Mechanical Engineering Science

Honorary Editor-in-Chief: Kuangchao Fan

Editor-in-Chief: Zhaoyao SHI

Associate Editors: Jinliang XU Yan SHI Jianlian CHENG

Editorial Board Members:

Haihui CHEN	Ailun WANG	Chun CHEN	Chunlei YANG	Yuliang ZHANG
Yajun HUI	Jigang WU	Liangbo SUN	Fanglong YIN	Wei LIANG
Weixia DONG	Hongbo LAN	Wenjun MENG	Xi ZHANG	Wanqing SONG
Shilong QI	Yi LI	Qiang JIANG	Yunjun LIU	Fei GAO
Yongfeng SHEN	Daoguang HE	Yi QIN	Xiaolan SONG	Jianbo YU
Hui SUN	Qingyang WANG	Guodong SUN	Xiaolong WANG	Yong ZHU
Jianzhuo ZHANG	Qingshuang Chen	Jianxiong YE	Kun XIE	Shaohua LUO
Mingsong CHEN	Jun TIAN	Qinjian ZHANG	Jingying SUN	Jiangmiao YU
Dabin CUI	Jing WEI	Daoyun CHEN	Jianhui LIN	Zhinan YANG
Wenfeng LIANG	Hongbo YAN	Yefa HU	Cai YI	Suyun TIAN
Hua ZHANG	Lingyun YAO	Xiangjie YANG	Zhijian WANG	Ying LI
Jianmei WANG	Peiqi LIU	Chunsheng SONG	Yeming ZHANG	Kongyin ZHAO
Xiaowei ZHANG	Wei LIU	Honglin GAO	Zhichao LOU	Yanfeng GAO

VISER

Publisher: Viser Technology Pte. Ltd.

ISSN: 2661-4448(online)

2661-443X(print)

Frequency: Semi-annual

Add.: 21 Woodlands Close, #08-18

Primz Bizhub SINGAPORE (737854)

https://www.viserdata.com/

Editors:

Yajun LIAN Yanli LIU

John WILSON Nike Yough

Mart CHEN Qiuyue SU

Debra HAMILTON Xin DI

Jennifer M DOHY Xiuli LI

Edward Adam Davis

Designer: Anson CHEE

Copyright © 2023 by authors and Viser Technology Pte. Ltd.

Mechanical Engineering Science

Volume 5 No.1 (2023)

CONTENTS

VISER

Special issue message

With the development and progress of science and technology, the speed of updating mechanical products has been accelerated. In the past, large-scale production was mainly used in the manufacturing of mechanical products, and the products were relatively single. Currently, small batch processing mode is often used in the implementation of mechanical product processing to ensure product diversity. To ensure the profits of production enterprises, attention should be paid to shortening the production cycle of mechanical products and minimizing production costs while ensuring quality. By implementing optimized design, the above goals can be met, reducing production time and costs to a certain extent, and seizing the market through efficiency.

In this issue, six papers will be published to evaluate the strength, stiffness, stability and other performance of mechanical structures through research and analysis of their construction and mechanical characteristics, in order to design and optimize mechanical structures reasonably. The methods proposed in this journal can be widely applied in various fields, optimizing the design of mechanical structures, improving the actual performance of machinery, shortening the working time of machinery, improving the efficiency and quality of machinery, effectively shortening the production cycle of products, increasing the actual production quantity of enterprises, providing more support for the further development of enterprises, and promoting the development of the mechanical manufacturing industry, which has certain practical significance.

Planner Author

Guangchen XU, master's degree, associate professor, was selected as a member of the Youth Expert Group of the Fluid Control Engineering Professional Committee of the Chinese Society of Mechanics in the Liaoning Province "Hundred and Ten Thousand Talents Project" (at the level of ten thousand people) in 2017.I graduated from the School of Mechanical Engineering, Zhejiang University of Technology with a Master's degree in Mechanical Manufacturing and Automation in 2010. I joined Yingkou Institute of Technology in the same year and currently serve as the Director of the Mechanism Teaching and Research Office of the School of Mechanical and Power Engineering. Main courses: Fundamentals of Mechanical Engineering Control, Mechanical Engineering Testing Technology, Detection and Control Technology, 3D Digital Modeling, etc. Research direction: Modeling and optimization of machine tool dynamics. Hosted and participated in 5 natural science foundation projects in Liaoning Province; Hosted three research projects at the college level at Yingkou Institute of Technology; Received one third prize of Liaoning Province Natural Academic Achievement Award and two third prizes of Yingkou City Natural Academic Achievement Award; In the past five years, more than 20 academic papers have been published, including 6 indexed by SCI and EI; Authorized 3 utility model patents and 3 software copyrights. Hosted one project of collaborative education between industry and academia by the Ministry of Education, one project of the 13th Five Year Plan for Education and Teaching in Liaoning Province, and two school level educational reform projects at Yingkou University of Technology; The course "3D Digital Modeling" hosted was awarded the provincial first-class undergraduate course in 2020; The textbook "Pro/E5.0 Mechanical Design and Application" edited by the editor won the first Liaoning Province Textbook Construction Award and participated in the compilation of 6 textbooks.

About the Author

Yuning SONG received his bachelor's degree and master's degree in Mechanical and electronic Engineering from Liaoning Engineering and Technical University in July 2007 and 2012 respectively, and his doctor's degree in mechanical Design and Theory from Liaoning Engineering and Technical University in January 2018. Presided over 2 science and technology research fund projects of Liaoning Provincial Department of Education, and participated in 1 project; Presided over 1 Natural Science Foundation Guidance plan of Liaoning Province, and participated in 5 projects; Presided over 1 regional joint innovation fund of Liaoning Provincial Natural Science Foundation, and participated in 5 projects; Presided over the 2023 Open Research Fund of the National and Local Joint Engineering Research Center for Mine Hydraulic Technology and Equipment; Presided over 1 excellent Science and Technology talent project of Yingkou Institute of Technology. The research proposes by referring to all kinds of research data and summarizing the analysis and research of various kinds of distribution disks, a new type of distribution disc with double V-shaped unloading slots is designed again. Then, the new designed disk is loaded into the piston pump by CFD software to simulate. Finally, through simulation, it is concluded that the width of the triangle slot of the distribution plate is about 10 °, the slope angle is about 12 °, and the diameter of the unloading hole is about 0.8mm. When the diameter of the perforated hole is about 1.5mm, the flow curve of the unloading hole is the smoother. Pressure shock and noise are also minimized at this time. Draw By improving the damping tank, the flow noise and cavitation change are smaller than before. He is currently the director of the Mechanical and Electrical Research Section of Yingkou Institute of Technology, and has won the title of Teacher Ethics Model, Excellent Communist Party Member and Excellent Teacher of Yingkou Institute of Technology for many times; Liaoning Province "ten million" talent project "ten thousand" level; Member of young Expert Group of Fluid Control Engineering Professional Committee of Chinese Mechanics Society; It has won 1 third prize of Science and Technology Award of China Federation of Commerce-National Commercial Science and Technology Progress Award; 1 third prize of Liaoning Provincial Natural Academic Achievement Award, 1 first prize and 2 third prize of Yingkou Natural Academic Achievement Award; participated in application and obtained 5 authorized utility model patents and 2 authorized software Copyrights; reviewed expert of Control Engineering; 1 academic monograph and project funding of Liaoning Provincial Excellent Academic Publication of Natural Science; published more than 20 academic papers in core journals, including 2 SCI papers and 3 EI papers. At present, he is mainly engaged in the modeling and simulation research of mechanical systems.

Meili YU, female, born in 1984, now works in Yingkou Institute of Technology, teacher, mainly engaged in graphics and design simulation research.

About the Author

Wenwu ZHANG, male, master's degree, senior engineer, associate professor, the 14th Outstanding Science and Technology Worker of Liaoning Province, and a candidate for the "Thousand" level of Liaoning Province's million person project. Graduated with a master's degree in 2016. I worked in the design, research, and management of CNC machine tools after graduating from 2005 to 2017. Since 2017, I have been working in universities and have been engaged in teaching and research in mechanical engineering for a long time. Published over 10 academic papers, including 3 SCI and EI indexed papers. Hosted the first set of products in the key field of provincial-level equipment manufacturing, won 3 provincial and ministerial level scientific and technological progress awards, and was granted 4 Chinese invention patents.

Lin QIAN, female, master's degree, engineer. Mainly engaged in the design, research and development of CNC machine tools, and published more than 10 academic papers, including 3 SCI and EI indexed papers. Hosted the first set of products in the key field of provincial-level equipment manufacturing, and obtained 3 authorized invention patents. All scientific research and technology are transformed into industrial applications, serving the development of the industry and generating significant social and economic benefits.

Qian WANG, an engineer. Born on February 21, 1986, I joined Yingkou Institute of Technology in 2011 and engaged in metalworking internship and casting training. Hosted and participated in 6 horizontal research projects at the college level; Participated in one longitudinal project at the college level; Published 7 papers; Obtained two software copyrights. Her main research direction is mechanical design, manufacturing, and automation.

About the Author

Xin CHENG is a current student at Yingkou Institute of Technology, currently a sophomore majoring in Materials Forming and Control Engineering. Has strong organizational skills, practical skills, and a spirit of teamwork, a strong sense of social responsibility, is down-to-earth and willing to work, and actively seeks opportunities for training. I constantly improve myself and enhance my personal qualities, and have been awarded a third class scholarship in school.

Jialei ZHOU is a current student at Yingkou Institute of Technology. I am currently a sophomore majoring in Materials Forming and Control Engineering. During their school years, students worked hard and earned multiple honors. Including the "Three Good Students" of Yingkou Institute of Technology from 2022 to 2023, the second prize in the Fourth Yingkou Institute of Technology College Students Advanced Mapping Technology and Product Information Modeling Innovation Competition, and the National Inspirational Scholarship for Yingkou Institute of Technology from 2022 to 2023.

Haoyang Liu is a current student at Yingkou Institute of Technology. I am a junior student in Materials Forming and Control Engineering. During my time in school, I studied diligently and received multiple honors. Including the third prize in the second Liaoning Province Casting Technology Competition, the third prize in the Liaoning Province Emergency Rescue Innovative Design Competition for College Students, and the excellent award in the fifth Liaoning Province Undergraduate Material Forming Technology Creative Competition.

About the Author

Zhaowei MENG is a graduate student of Yingkou Institute of Technology. I am a student majoring in Mechanical Design, Manufacturing and Automation in the 2019 cohort. During school, I studied diligently and was good at communicating with others. Diligent and serious in learning, excellent in grades, excellent in character and learning, and a love for the collective have won multiple honors. Including the third prize in the second Liaoning Province Casting Technology Competition and the third prize scholarship from Yingkou University of Technology.

Liang HAN graduated with a master's degree from Chang'an University and is a senior engineer. Hosted 2 provincial-level scientific research projects, published 4 EI papers, and 2 Chinese core journals. Publish one monograph and two textbooks. My main research interests lie in mechanical dynamics, mechanical design, and vibration analysis in the field of machine tools.

Viser Technology Pte. Ltd.
Mechanical Engineering Science
DOI: 10.33142/mes.v5i1.12710

Research Article | Open Access

Design and Optimization of New Smoke Exhaust Pipe for Mining Trucks

Qian WANG, Cheng XIN, Jialei ZHOU, Liang HAN*

Yingkou Institute of Technology, Yingkou, Liaoning, 115004, China

***Corresponding Author:** *Liang HAN, E-mail: 312462525@163.com*

Abstract:
In order to improve the maintenance efficiency, extend the use time, ensure that the exhaust emission meets the standard, for the 830E truck heating bucket exhaust pipe design defects, the current single smoke exhaust system is transformed into a time period, convertible smoke exhaust system. After the transformation, it can not only realize the side row to prevent direct corrosion of the box bucket in summer, but also realize the heating of the box bucket at low temperature in winter to prevent snow and ice and frozen blocks from sticking to the box bucket and the materials transported. After the transformation can save a lot of manpower, material resources, financial resources, improve the service life.
Keywords: *smoke exhaust pipe; mining truck; extended use*

1 Background and Significance

The smoke exhaust system of 830E mining truck adopts the design of heated pipe exhaust pipe, and the smoke exhaust also has the role of heating. In winter, there is much rain and snow in northern China, and it is easy to freeze materials. Prevent material freezing through the heating of the exhaust pipe. But in summer, the heating effect is ineffective, and the smoke is washed all the year round, which is easy to cause the phenomenon of aging and corrosion inside the smoke pipe. In order to reduce the corrosion of the smoke exhaust system on the inner compartment, the current single heated compartment pipe exhaust system is transformed into a time period and convertible smoke exhaust system. Disconnect the original pipe below the platform, install the three-way pipe, and have the system conversion function. In this way, the mode of "smoke exhaust + heating" is adopted in winter, and the single smoke exhaust mode is adopted in summer, which reduces the smoke erosion by three quarters, which fundamentally improves the service life and reduces the failure rate.

2 Design Ideas

When needed, the smoke exhaust mode should be converted at will. The conversion should ensure the sealing of the changing chamber, and no smoke leakage in the closing direction. Smoke exhaust box change valve timely conversion; The transformation process takes into account the possible impact of the smoke exhaust system change on the engine power, To design it properly, Reasonable layout; The transformation process should fully consider the impact of the change of the smoke exhaust system on the temperature environment change around the engine smoke exhaust pipeline, To arrange the pipe layout of the smoke exhaust pipe reasonably, To achieve the minimum impact on the surrounding pipeline; The modification scheme shall fully consider the existing installation position of the left and right diesel tank and hydraulic fuel tank, During the renovation process, Keep a safe distance from all pipes on the car; Smoke exhaust system transformation of all materials using high-temperature resistant materials, Use of ferrite stainless steel; For the minimum transformation of the original exhaust pipe, The modified interface should be consistent with the existing smoke exhaust interface.

The layout and method of the 830E truck exhaust pipe before the transformation are as follows:

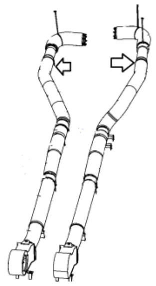

Figure 1 The layout diagram of the front row pipe

Copyright © 2023 by author(s) and Viser Technology Pte. Ltd. This is an Open Access article distributed under the terms of the Creative Commons Attribution-NonCommercial 4.0 International License (http://creativecommons.org/licenses/by-nc/4.0/), permitting all non-commercial use, distribution, and reproduction in any medium, provided the original work is properly cited.
Received on April 7, 2023; Accepted on May 11, 2023

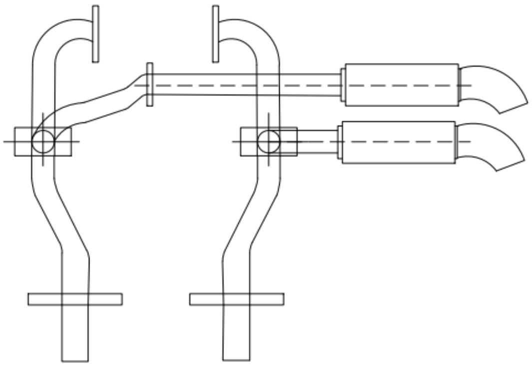

Figure 2 The layout diagram of the smoke exhaust pipe after the renovation

3 Specific Methods

(1) Location selection. Smoke pipe front for engine related smoke parts, quantity, complex structure, transformation space is very limited, so the front add side is difficult, then after the pump concentration area, pipeline, considering safety factors, is also unfavorable to add side, so choose in the middle, the rear support beam bridge selection position add side device is the most reasonable, the middle pipe completely modified, from the original exhaust pipe front interface connection, high and low parallel arrangement, fixed installation on the right side of the platform.

(2) Function implementation. In completely reserved before and after the smoke pipe case, the middle exhaust pipe (support interface after the beam to the main first interface) for modification, this section add or redesign a tee tube, respectively connect the front, back and side device, and the tee pipe has the valve can respectively realize the front-three-back-front-three-side device corresponding smoke function, to achieve the purpose of free switch.

(3) Related parameter design of smoke exhaust pipe: ①straight section span smoke exhaust pipe, the material is aluminized steel, surface spraying rust prevention, corrosion prevention, high temperature resistance and other polymerization materials, groove inner diameter of $\varphi_{concave}$=240 mm, convex along the outer diameter φ_{bulge}=235 mm, outer edge diameter $\varphi_{outside}$=250 mm, two lengths and sizes, short pipe L_{short}=500mm, long tube L_{long}=2450 mm, the groove and the convex edge form a groove connection mode, the outer edge surface is fastened by a clamp, the two end of the section of the pipe is the groove surface, and the other end is the convex edge surface.②The middle three-way exhaust pipe, T-shaped three-way pipe, the material uses the same straight span pipe, the front and rear ends are respectively groove, convex edge design, the vertical end has no processing process, each diameter is the same as the straight section exhaust pipe, the length of each end is $L_{Through}$=430 mm, a leaf surface valve device is designed and installed at the rear end and the vertical end of the three links. The external control mechanism can effectively drive the valve to rotate 360°, and the leaf surface can open or close the channel with the rotation, so as to achieve the purpose of changing the direction of smoke exhaust fluid.③90°bent smoke exhaust pipe, the main function is to change the three-way vertical end direction to the silencer, so that the smoke exhaust direction changes from vertical to horizontal to right. Its design parameters are: bending angle DOB value is 90°, space angle POB value is 283°, and each diameter angle is the same as the above smoke exhaust pipe.

Figure 3 Physical drawing of reversing room

Figure 4 Overall physical drawing of row of smoke pipe

4 Related Accessories

4.1 Fire proof cloth

Transformation process to fully consider the smoke system to the engine exhaust pipe surrounding the temperature of the environment changes, to reasonable layout of smoke pipe layout, to do minimum influence, the surrounding pipe fire need to measure custom, after the modification of fire cloth bandage not cracks should be completely fit, fire cloth should have protective layer, heat insulation layer, appearance oil high temperature resistant silicone fire layer, insulation cotton thickness is not less than 2.5cm, fire bag cloth with high temperature resistant ceramic fiber cotton, fiber cloth, steel wire mesh, heat insulation nails according to the modification of the smoke pipe shape.

Figure 5 Fire protection cloth

4.2 Silencer

Figure 6 Silencer

Resistance silencer, the straight tube multi-chamber structure is suitable for large smoke flue, its principle is the use of porous and related sound-absorbing materials to reduce the noise, in the process of acoustic transmission, the pipe cross-sectional area or internal resonance chamber can cause the change of acoustic impedance, sound energy reflection and consumption, sound absorption material fixed in the smoke circulation wall or the resonance chamber, when the sound wave into the silencer, part of the sound energy in the pores of the porous material and friction into heat dissipation, sound wave weakened. The muffler has a good effect on high frequency noise. The internal material is 2 mm thick high temperature resistant, corrosion resistance metal plate, the surface is perforated and rolled into a cylindrical, the pore diameter is about 5mm, the perforation rate is about 60%, the external surface is still the same straight span pipe material, processed into chamber welding and inner surface welding, the design size is: inner pipe diameter φ_{inner}=240mm, outer tube diameter of $\varphi_{outside}$=400mm, silencer length L elimination =1420mm.

5 Full Text Summary

Through the design and transformation, the service life of the exhaust pipe is improved, the service time of the 830E mining truck exhaust system is longer, the service life of the truck exhaust pipe is more than 20,000 hours, the maintenance cost is reduced, and a lot of manpower, material resources and financial resources can be saved after the transformation.

Fund Project: (1) 2022 Liaoning Natural Science Foundation Plan (Yingkou Joint Fund) Damping damping Design and Optimization of New Bore Head Transmission Structure (Fund No.: 2022-YKLH-17); (2) In 2023, the key scientific research project of Yingkou Institute of Technology is the Design and Optimization of Smoke Drainage Pipe for New Mining Truck (Fund No.: ZDIL202306); (3) 2021 Natural Science Foundation of Liaoning Province (Yingkou Joint Fund) Research on Dynamic Characteristics of Damped Dynamic Reduction Vertical Holack (Fund No.: 2021-YKLH-08).

References

[1] Xie Xiaomei. Optimization of ship engine room smoke exhaust pipe support design [J]. Journal of Qingdao Vocational College, 2021.3:66-75.

[2] Cao Jijun. Study on the vibration characteristics of smoke exhaust pipe of ship main vessel [D]. Dalian University of Technology, 2016.

[3] Huang Yilong, Zhang Shaogang, Shi Yanli. Analysis on the improvement effect of the lateral smoke exhaust efficiency of the distributed smoke exhaust pipe [J]. Fire Protection Science and Technology, 2022.4:107-130.

[4] CAI Xiaotao, Dong Jiahuan, Huang Zhiwu ,et al.. Vibration reduction design of the main engine smoke exhaust pipe system of the scientific research vessel [J]. Ship Engineering, 2022.11:35-42.

Viser Technology Pte. Ltd.
Mechanical Engineering Science
DOI: 10.33142/mes.v5i1.12711

Research Article Open Access

Design of Damping Damping Design of New Boring Head Drive Structure

Haoyang LIU, Zhaowei MENG, Liang HAN*, Wenwu ZHANG

Yingkou Institute of Technology, Yingkou, Liaoning, 115004, China

***Corresponding Author:** Liang HAN, E-mail: 312462525@163.com*

Abstract:
This paper takes the boring head of 20 roll mill as the research object, optimizes the vibration inside the boring head through a differential damping structure, and then conducts the 3 d model inside the boring head through SolidWorks, and checks the interference of the boring head model. Finally, Ansys workbench finite element analysis software is used to analyze and verify the vibration damping characteristics of the differential damping structure.
Keywords: *Gear drive; Damping; Vibration Reduction*

1 Background and Meaning

With the progress of science and technology and the rapid development of machining technology, the quality requirements of the parts are also improved. The structure of too complex parts make the traditional processing process can not meet. The precision of some holes is more demanding. Due to the increase of space surface roughness of the boring head, the optimization design of the boring head is needed. At the same time, the mechanical system is developing towards the direction of diversification, intelligence and flexibility, and the topic of vibration reduction has increasingly become one of the important research topics at home and abroad.

In the process of gear transmission, due to the change of time-varying meshing stiffness, transmission error, in and out impact, and the change of the system input and output torque, the alternating load will cause the engagement impact of the gear. When the frequency of the shock force is close to the inherent frequency of the gear, it will cause resonance and noise [1].

Circumferential vibration, radial vibration and axial vibration are the three ways of gear vibration. Due to the error of the gear and the different changes of the gear engagement stiffness, the vibration of the shaft and bearing, which causes the vibration of the gear in the radial direction of the gear. Secondly, when the tooth load is applied on the bearing, due to the bending deformation of the shaft, the axial force caused by the friction between the shaft and the bearing is not consistent at the left and right ends of the gear, thus causing the axial vibration of the gear [2]. That is to say, both radial and axial vibration are generated by circular vibration as the starting factor.

Through reading a series of references, we learned that the common methods of vibration reduction are active design and passive vibration reduction. Active design is to optimize the existing parameters of the wheel to improve the machining accuracy of the work piece, while passive vibration reduction is to control the gear through other physical methods after the production of the finished product. One of the most effective methods today is to use damping rings for passive gear damping. The damping ring is embedded in the gear. When the transmission system begins to operate, the damping ring and the matching gear produce sliding friction. The principle of energy consumption between the sliding friction between the two, so as to reduce the vibration between the transmission system and realize the effective control of the gear vibration.

2 Main Research Content

2.1 Design of differential damping and damping structure

In this study, the speed difference between the driven gear and the damping gear is mainly used to produce friction, and the mechanical energy in the friction loss mechanism can achieve the effect of system vibration reduction. There are many structures of wheel damping ring, mainly integral, C-shaped and spiral

Copyright © 2023 by author(s) and Viser Technology Pte. Ltd. This is an Open Access article distributed under the terms of the Creative Commons Attribution-NonCommercial 4.0 International License (http://creativecommons.org/licenses/by-nc/4.0/), permitting all non-commercial use, distribution, and reproduction in any medium, provided the original work is properly cited.
Received on April 7, 2023; Accepted on May 13, 2023

damping ring. When the gear vibrates, the relative sliding movement between the gear and the damping ring occurs, that is, there is sliding friction force. Using the energy consumption principle of sliding friction force, the mechanical energy of the gear vibration is converted into the heat energy caused by friction, so as to reduce the vibration energy of the gear and achieve effective control of the vibration of the gear. However, the design of the damping ring involves many factors, because all the damping rings are generated by the relative friction movement between the ring and the gear body ring groove. The size of the friction force determines the damping effect of the ring [3]. If the friction between the damping ring and the gear is very small, even does not exist, the damping ring and the gear become two unrelated motions, the damping ring can not suppress the vibration of the gear; if the friction force is particularly large, the damping ring will move with the gear without the relative movement, which can not form friction energy consumption [4]. To solve this problem, a tooth differential damping structure is developed, as shown in Figure 1.

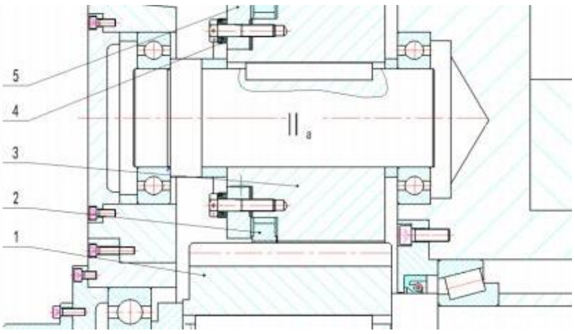

Figure 1 Diagram of differential damping damping structure

1, spindle drive gear; 2, damping gear; 3, shaft drive gear; 4, disc spring set; 5, spring pressure cover;

The damping vibration reduction structure is the process of gear engagement, the driven gear is composed of two gear body, namely damping gear 2 and shaft transmission gear 3, because the number of damping gear 2 one more teeth than the shaft transmission gear, so the boring head working process, small speed difference between damping gear 2 and shaft transmission gear transmission 3, thus forming the sliding friction between the two gears, the sliding friction to consume the mechanical energy generated by vibration in the system, so as to reach the effect of vibration reduction. By adjusting the compression amount of the butterfly spring 4 on the damping pressure cover 5 in contact with the damping gear, the damping force effect of the damping gear can be changed.

2.2 Dimensional modeling and assembly of boring head parts

The SolidWorks software is used for 3D modeling of the boring head parts and simulated assembly to better express the "148" structure transmission layout of the boring head parts, as shown in Figure 2.

Figure 2 The 3 D model diagram of the boring head

The structure of boring head parts is complex and there are many kinds of parts. If there is no interference inspection on the three-dimensional model of boring head assembly, there may be hidden danger of collision teeth and other parts in the later factory processing. The interference inspection can effectively reduce and minimize our loss. Although the traditional interference inspection of parts drawings can find a certain amount of interference parts, but the efficiency is low and easy to miss. Therefore, this paper uses the "interference check" module of Solidworks software to calculate the interference inspection of the boring and head parts after simulated assembly. The place with interference is marked as shown in Figure 3. After the interference position is gradually eliminated, and then checked to ensure that the 3 D drawing is completed without interference.

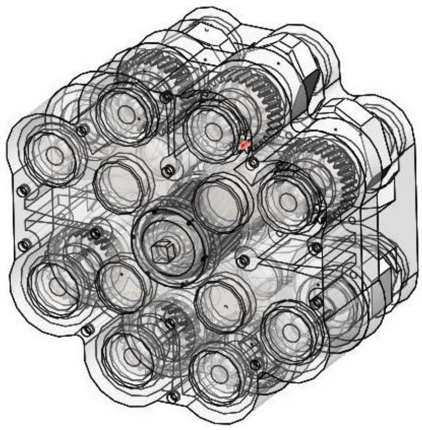

Figure 3 Interference gram of 3D model of boring head

2.3 Comparison of shock effect of differential damping structure

According to the calculation, the damping force of the differential transmission damping structure can be controlled by adjusting the butterfly spring compression or replacing the friction damping material between the damping gear and the transmission gear. The damping force of this structure is easy to adjust and the damping force is constant and reliable. In the setting of the damping force, this paper extracts a pair of meshing gears in the boring head, and calculates the vibration reduction characteristics of the Damping ring on the axial Vibration of the gear system published by the domestic scholar Qingyang Wang and others.

Before optimization, the gear engagement is analyzed, the active gear and driven gear are selected, and a constraint is applied on the active gear to make it engage. Through the overall vibration displacement image, the maximum vibration displacement of the gear engagement is 0.01283mm. After optimization, the damping gear is added before the driven gear, the butterfly spring in front of the damping gear, and the transmission system is analyzed to find the minimum vibration displacement of the gear when the damping force is 561.845N, and the vibration displacement during the engagement is 0.002496mm, which can effectively explain the vibration reduction results, as shown in Figure 4 and Figure 5:

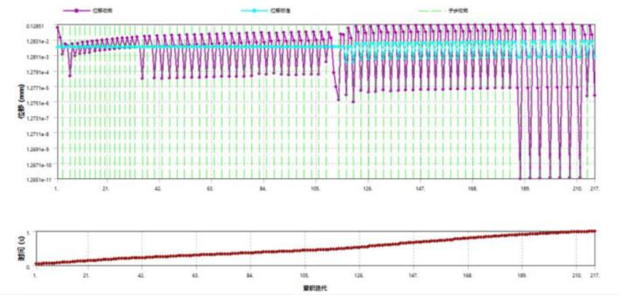

Figure 4 Graph of vibration displacement convergence during unoptimized front gear engagement

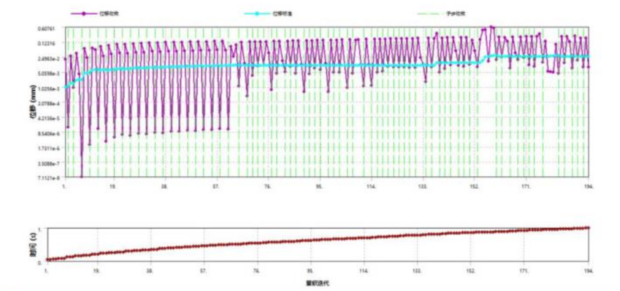

Figure 5 Convergraph of vibration displacement during optimized gear engagement

3 Summary of this Article

According to the problem of machining of mill frame, a special boring head of 20 roll mill frame is developed, which aims 8 holes of the machining hole system with a walking blade. The "gear-damping" vibration reduction system is applied to produce a better processing effect. This method is based on the gear in the original transmission system, plus a damping gear, damping gear than a gear number, so in the process of transmission, there is a certain speed difference between damping gear and transmission gear, further form sliding friction, reuse sliding friction energy consumption principle, consumption vibration generated mechanical energy, so as to achieve the effect of vibration reduction. At the same time, the amplitude of the boring head transmission system changes nonlinear with the damping force, through the simulation model of the transmission system.

Fund Project: (1) 2022 Liaoning Provincial Natural Science Foundation Plan (Yingkou Joint Fund), New Style Design and Optimization of Bore Head Drive Structure (Fund No.: 2022-YKLH-17). (2) In 2023, the key scientific research project of Yingkou Institute of Technology is the Design and Optimization of Smoke Drainage Pipe for New Mining Truck (Fund No.: ZDIL202306). (3) 2021 Natural Science Foundation of Liaoning Province (Yingkou Joint Fund) Research on Dynamic Characteristics of Damped Vertical Shack (Fund No.: 2021-YKLH-08).

References

[1] Zhong Yantao, Wang Liqin, Li Wenliang, et al.. Research on damping and damping technology of gear transmission [J]. Mechanical transmission, 2011,35(11):17-20.

[2] Yan Shaoxia, Su Ronghua. Experimental study on vibration reduction and noise reduction of gear damping ring [J]. Construction Machinery, 1995(2):19-20.

[3] Huang Hongliang, Li Guilin, Ou Daisong. Design and analysis of damping damping ring of aviation bevel gear [J]. Aero-engine, 2013,39 (2):25-30.

[4] Feng Haisheng. Dynamic characteristics of high speed and high power density gear transmission system and damping ring damping research [D]. Harbin Institute of Technology, 2015.

Viser Technology Pte. Ltd.
Mechanical Engineering Science
DOI: 10.33142/mes.v5i1.12712

Research Article Open Access

Research and Analysis of Shear Performance of Inclined Blade Shears Based on ANSYS

Meili YU*, Guangchen XU

Yingkou Institute of Technology, Yingkou, Liaoning, 115014, China

***Corresponding Author:** Meili YU, E-mail: 263042809@qq.com*

Abstract:
Nowadays, enterprise customers have higher and higher requirements for steel plate quality, and the performance research of shearing machine has been widely paid attention to. In this paper, the finite element analysis software ANSYS is used to analyze and verify the key parts of the downcut inclined blade shears. Through continuous analysis and improvement of the model, the weak points are optimized to improve the shear performance and production efficiency of the shears.
Keywords: *ANSYS; Shear quality; Shear property*

1 Introduction

As one of the key equipment in metal sheet and strip production line, the performance of shearing machine directly affects the production cost and product shearing quality. Many scholars have studied the performance of different types of shears through mathematical modeling and simulation, and achieved important results. Among them, Xu Kuan [1] et al. established a three-dimensional disk shear model based on the finite element method. The Gissmo material failure criterion is introduced to calculate and analyze the stress on the upper cutting edge under different lateral clearance, overlap amount and the upper cutting edge Angle. The results show that the upper cutting edge Angle has the most obvious influence on the stress on the upper cutting edge, and the stress on the upper cutting edge decreases with the increase of the upper cutting edge Angle. Chen Baosong [2] from Shanghai Baosteel Construction Engineering Design Co., LTD., analyzed the stamping defects caused by disk shear, and took optimization measures in the aspects of disk shear side clearance, overlap amount, material and daily maintenance, which greatly improved the strip quality and processing efficiency with remarkable results. Wang Zhenhong [3] also optimized the structure of the roller cutting shears, whose optimization object was the upper edge of the shears. In the research process, structural topology was adopted to analyze the mechanical properties of the upper edge knives, and then its optimization performance was realized. Nowadays, enterprise customers have higher and higher requirements for steel plate quality, and the performance research of shearing machine has been widely paid attention to. Based on the current research situation at home and abroad, it is concluded that there are not many researches on the downcut inclined blade shearing machine. Through analyzing different research methods and contents, it is necessary to study the performance of the inclined blade shearing machine, which is also a supplement to the past research. It also plays a certain reference role for the performance improvement and optimization design of the same type of heavy equipment.

2 Theoretical Analysis and Calculation

The object of this study is a hydraulic downcut inclined blade shear machine of an enterprise, and the frame is welding parts, so it has enough stiffness to prevent damage in the operation. When working, the upper cutting edge does not move, and the lower cutting edge moves up and down with the lower tool holder under the thrust of the hydraulic cylinder, and the work advance and fast retreat are constantly carried out, and the stroke is controlled by the hydraulic cylinder. At the same time, the lower cutting edge is installed at a small Angle to reduce the deformation degree of the cut strip. The mechanism diagram of the undercutting inclined blade shears is shown in Figure 1.

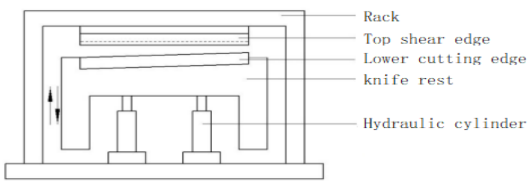

Figure 1 Schematic diagram of the mechanism of the undercutting oblique blade shears

Copyright © 2023 by author(s) and Viser Technology Pte. Ltd. This is an Open Access article distributed under the terms of the Creative Commons Attribution-NonCommercial 4.0 International License (http://creativecommons.org/licenses/by-nc/4.0/), permitting all non-commercial use, distribution, and reproduction in any medium, provided the original work is properly cited.
Received on April 7, 2023; Accepted on May 22, 2023

2.1 Calculation of shear force

Because the cutting edge is installed at an Angle, when cutting, the cutting edge and the plate contact only a part of the section. For shear force, this study uses BB Nosari's calculation formula commonly used at present [1]. The total shear force consists of three parts: P=P1+P2+P3, where P1 is the pure shear force; P2 is the bending force of the part of the upper cutting edge that has been cut during shearing. P3 is the bending force required to bend the metal near the incision.

2.2 Determination of working pressure of hydraulic cylinder

Table 1 Commonly used working pressure of various types of hydraulic equipment

Device type	General machine tool	General metallurgical equipment	Agricultural machinery, small construction machinery	Hydraulic press, heavy machinery,Rolling mill push down lifting machinery
Working pressure(MPa)	1～6.3	6.3～16	10～16	20～32

As the power source, the hydraulic cylinder transmits the thrust of the hydraulic cylinder to the cutting edge through the cooperation of various institutions, so as to complete the shear movement. In this topic, the hydraulic downward cutting oblique cutting edge shear machine adopts the hydraulic direct pushing type. Since the upper cutting edge is fixed on the frame and does not move, the hydraulic cylinder pushes the cutting edge to move up and drive the cutting edge to complete the shear. Therefore, the load that the hydraulic cylinder needs to bear in addition to the shear force should also include the gravity of the lower tool holder and the cutting edge, the material of the shear machine has been determined, the theoretical weight of the tool holder is 145kg, and the theoretical weight of the cutting edge is 5kg. The shear force is calculated and the total load required by the two hydraulic cylinders is finally obtained. According to the above table, the working pressure of the hydraulic cylinder can be selected as 14MPa.

3. Cutting Edge Optimization Design of Shearing Machine

3.1 ANSYS finite element analysis of cutting edge

The cutting edge material selected in this paper is 5CrW2Si, which has good hardenability and high temperature mechanical properties [4]. The cutting edge is tightened by 10 bolts and completely fixed on the lower tool holder. The overturning moment in the shearing process mainly acts on the bolts. When cutting the material, the cutting edge and the tool holder can be regarded as one, and the guide rods on both sides are fixed to move up and down continuously, and the plane position does not change, so the nodes on the surface of the 10 bolt holes are completely fixed. The external load on the cutting edge can be directly applied to the maximum shear force of the system pressure, so that the results can be obtained within the safe range. The moving load P (that is, the shear force) acts on the edge of the cutting edge, moving from the left side to the right side, and its magnitude and direction always remain the same.

In this analysis, the whole process is divided into 10 parts, each subject to a downward shear force, one part of the force, the rest of the force is not. The whole step is divided into 10 steps, the load from left to right in turn on the ten small planes, until the last plane, the shear step is completed. The maximum strain and maximum equivalent stress of each loading step can be obtained by calculating and analyzing the moving load acting on each small plane in turn, as shown in Table 2.

Table 2 The maximum deformation and equivalent stress of the cutting edge under each load step

Load steps	1	2	3	4	5	6	7	8	9	10
Max deformation/ 10^{-2}mm	5.16	2.58	2.58	3.24	3.28	3.22	3.24	2.56	2.60	5.12
Max equivalent stress/MPa	182	94	113	143	138	133	114	110	109	175

It can be seen from Table 2 that the distribution of shear edge strain and equivalent stress is not uniform on the whole. Since the deformation in operation belongs to elastic deformation, the distribution of the equivalent stress and equivalent strain of the shear edge can be regarded as the same trend. By comparing the shape and equivalent stress of the cutting edge under different loading steps, it can be found that the equivalent stress of the cutting edge changes most obviously at the first loading step. The maximum equivalent stress and deformation of the cutting edge occur at both ends, and the specific values are 182.2MPa and 0.0516mm respectively. The equivalent stress and deformation within the left and right ends of the cutting edge are the smallest.

Analysis of the calculation results shows that:

(1) The deformation is mainly in the horizontal Y direction, and the deformation in the X direction and the Z direction is relatively small;

(2) The blade is bent to both sides as a whole, and the deformation at the bend is relatively large;

(3) Under moving load, the maximum equivalent stress on the cutting edge is 182.2MPa, located at the bolt holes at both ends of the cutting edge, and the maximum yield limit of the cutting edge is 1920MPa, so the cutting edge is in a safe state.

3.2 Cutting edge optimization design

On the premise of meeting the design conditions, taking the strength limit as the constraint and improving the shear performance of the shear machine as the goal, the method of improving the structure of the shear edge is as follows: by improving the structure of the shear edge, the equivalent stress and deformation of the shear edge are calculated by finite element analysis. The specific methods include: increasing the thickness of the cutting edge, increasing the thickness of the bolt hole, chamfering the corners at both ends of the cutting edge, etc. Therefore, the structural improvement scheme is proposed as shown in Table 3, and the finite element analysis and verification are respectively carried out as shown in Table 4.

Table 3 Structural improvement parts of each plan

option	Improve the parts and contents
Option one	The cutting edge thickness was increased from 30mm to 35mm
Option two	Bolt hole thickened from 8mm to 14mm
Option three	Round the corners of the two ends of the cutting edge by 20mm

Table 4 Comparison of cutting edge structure improvement schemes

option	Max deformation		Max equivalent stress	
	Numerical value/mm	Rate of change/%	Numerical value/MPa	Rate of change/%
Primary structure	0.0516	—	182.17	—
Option one	0.0486	-5.81	184.22	+1.13
Option two	0.0346	-32.9	118.48	-35.0
Option three	0.0458	-11.2	177.25	-2.70

Through analysis, it is concluded that increasing the overall thickness of the cutting edge can only reduce the maximum deformation, but the maximum stress will increase, and the weight of the cutting edge will also increase, resulting in higher requirements for the hydraulic cylinder of the power plant. If scheme 2 is used to increase the thickness near the bolt hole, the maximum deformation and maximum stress will be reduced, and the amplitude is large, while the weight of the cutting edge will increase but not much, and the impact is not large. When scheme 3 is used to chamfered the corners of both ends, the maximum deformation and maximum stress will also be reduced, and the weight will be reduced, but the shear stroke will be increased, affecting the improvement of shear efficiency.

4 Optimization Design of Lower Tool holder of Shearing Machine

4.1 Statics analysis of lower tool holder

The tool holder of the shearing machine is a welding part, and the analysis will be too complicated if the relationship between the welded parts is considered, so the simplification is carried out under the condition of meeting the characteristics of the model. The tool holder material is Q235. Add constraints: The tool holder is connected to the hydraulic cylinder by bolts. Since the hydraulic cylinder works synchronously, there is no plane movement and rotation during the operation, so the nodes on the bottom bolt hole surface are completely fixed. Applied load: The external load on the shearing machine can directly adopt the maximum shear force of the system pressure, which can make the result within the safe range. The moving load (that is, the shear force) acts on the tool holder, moving from the left side to the right side, and the size direction is always unchanged. At the same time, the shear machine is subjected to upward thrust from the hydraulic cylinder. The deformation and equivalent stress distribution of each load step can be obtained through solving, as shown in Table 5.

Table 5 Maximum deformation and equivalent stress of tool rest under each load step

Load steps	1	2	3	4	5	6	7	8	9	10
Max deformation/ 10^{-3}mm	12.0	4.98	2.91	2.69	3.68	3.74	2.77	2.57	5.54	14.4
Max equivalent stress/MPa	9.96	6.28	4.74	7.38	7.51	8.25	8.50	5.27	6.12	12.2

It can be seen from Table 5 that the strain stress distribution of the tool holder is not uniform, and since the deformation during operation belongs to elastic deformation, the distribution trend of the two is the same. At the 10th loading step, the equivalent stress and strain values are the largest, which are 12.2MPa and 0.0144mm, that is, the connection between the beam and the two legs is the weak point of the structure. Figure 2 and Figure. 3 show the maximum deformation and maximum isoeffect diagram at the 10th loading step.

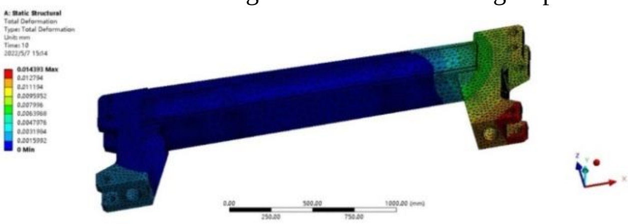

Figure 2 Tool rest deformation diagram (load step 10)

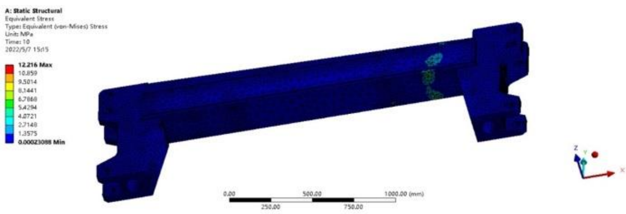

Figure 3 Effect diagram of tool rest (load step 10)

By analyzing the results, it can be found that:

(1) The deformation mainly occurs in the horizontal X direction, and the Y direction and Z direction are relatively small;

(2) The whole tool holder is bent to both ends, and the deformation on both sides is larger;

(3) The maximum equivalent stress of the tool holder is 12.2MPa, which is located at the bottom bolt hole, and the yield limit of the tool holder is 235MPa, so the tool holder is in a safe state.

4.2 Optimization design of lower tool holder

In this paper, the optimal design method of the lower tool holder is the experimental verification method. The optimization design principle is: on the premise of meeting the design requirements, the maximum equivalent stress and deformation are calculated with the strength limit and the original deformation as constraints, so as to improve the shear performance of the shear machine. The specific structural improvement methods include: increasing the overall thickness of the tool rest, increasing the width of the tool rest legs on both sides, increasing the rib plate where the tool rest body is connected to the tool rest legs, increasing the height of the tool rest main part, moving the bolt hole at the bottom of the tool rest used to connect with the base to the interior, chamfering the edge line of the bolt hole, changing the size of the bolt hole, etc. By changing the structure of the tool rest, eight improvement schemes are proposed, as shown in Table 6.

Table 6 Structural improvement areas of each program

Option	Improve the parts and contents
Option one	The overall thickness of the tool holder is increased from 200mm to 250mm
Option two	The width of the legs on both sides is increased from 390mm to 450mm
Option three	Add a 50mm wide rib plate to the place where the main body of the tool holder connects to the leg of the tool holder
Option four	The main part of the tool holder is thickened 50mm from below
Option five	Move the bolt hole at the bottom of the tool holder inward by 15mm
Option six	Invert a 2mm Angle on the edge of the bolt hole
Option seven	Change the bolt hole to M18
Option eight	Change the bolt hole to M22

It can be seen from the analysis results in Table 7 that Option 2, 3, 5, 6 and 7 cannot optimize the tool rest. For the optimization of the structure, only Option 1, 4 and 8 need to be considered, that is, the overall thickness of the tool rest needs to be thickened. Thickening below the main part of the tool rest; Increase the size of the bolt hole. One of them can reduce the amount of deformation, but will increase some of the maximum stress, and will make the weight of the tool holder larger, thereby increasing the requirements for the hydraulic cylinder; Scheme four can greatly reduce the amount of deformation, but it will also increase some maximum stress, and the weight of the tool holder will also increase, but less than scheme one; Plan eight can reduce the amount of deformation, and can reduce the maximum stress, but the amplitude is not very large.

Table 7 Comparison of cutting edge structure improvement schemes

Option	Max deformation		Max equivalent stress	
	Numerical value/mm	Rate of change/%	Numerical value/MPa	Rate of change/%
Primary structure	0.0144	—	12.2	—
Option one	0.0136	-5.56	12.4	1.64
Option two	0.0146	1.39	14.8	21.3
Option three	0.0144	0	13.7	12.3
Option four	0.0114	-20.8	12.3	0.82
Option five	0.0157	9.03	12.9	5.74
Option six	0.0144	0	20.8	70.5
Option seven	0.0148	2.78	18.2	49.2
Option eight	0.0141	-2.08	12.0	-1.64

5 Conclusion

Through the analysis of the key parts of a company's bevel blade shears, it is concluded that in order to achieve the goal of improving the shear performance of the hydraulic bevel blade shears, the structure of the main parts of the hydraulic bevel blade shears can be improved by the following methods:

(1) Increase the thickness near the bolt hole of the cutting edge without affecting the installation of the cutting edge; Appropriately increase the overall thickness of the cutting edge with the thickness near the bolt hole to prevent excessive thickness from increasing the requirements on the hydraulic cylinder; The corners of both ends of the cutting edge are rounded in a small amplitude to prevent excessive chamfering from increasing the shear stroke and reducing the shear efficiency;

(2) The thickness under the main part of the tool holder is mainly increased without affecting the installation of the cutting edge; At the same time, the diameter of bolt hole should be increased appropriately. The overall thickness of the tool holder can also be thickened, but not too much to prevent the requirements of the hydraulic cylinder from being too high;

(3) Increase the thickness of the base where the cutting edge is fixed without affecting the installation of the cutting edge, increase the rib at the connection between the frame beam and the two columns, and appropriately increase the overall thickness of the frame, the width of the frame two columns and the height of the

frame beam to prevent excessive increase in the weight of the frame and increase its manufacturing cost.

Fund Project: 2021 Regional Innovation Joint Fund Project of Natural Science Foundation of Liaoning Province (2021-YKLH-13; 2021-YKLH-03).

References

[1] Xu Kuan, Xia Mingsheng, Liu Jingbao, et al. Simulation of disc shear blade Stress based on Gissmo Material failure criteria [J]. Journal of Plasticity Engineering, 2021,28(9):110-116.

[2] Chen Baosong. Optimization Analysis of Disc Cutting Device for Cold Rolling Strip Steel [J]. Shanxi Metallurgy, 2023, 46(4):227-229.

[3] Wang Zhenhong. Mechanism Optimization of Rolling Shear and Topological Optimization of Upper Tool Rest [D]. Dalian Jiaotong University, 2012.

[4] Melya Dyanasari Sebayang,Erlangga Kustyawan. Design of material transfer automation in shearing machine[J]. IOP Conference Series: Materials Science and Engineering, 2018,420(1):1.

[5] Xu Yunxiang. Optimization design of Hydraulic Brake shears frame based on ANSYS [D]. Shandong University of Science and Technology, 2018.

[6] Sheng Aijun, Yang Ruiyu, Chen Lunshu, et al. Structure Optimization of Medium and thick plate shear line Equipment [J]. China Heavy Equipment, 2022(2):13-15.

[7] Chen Baosong. Optimization Analysis of Disc Cutting Device for Cold Rolling Strip Steel [J]. Shanxi Metallurgy, 2023,46(4):227-229.

[8] Li Ping. Analysis of Factors influencing the shape control System of hot rolled strip head-and-tail shear [J]. Metallurgical Automation, 2019,47(S1):282-287.

[9] Dong Guiwei, ZHAO Guoqun, Yan Jun, et al. Development and application of Virtual simulation design system for tracking shears based on SolidWorks [J]. Experimental Technology and Management, 2021, 38(4):132-135,140.

[10] Bai Huijie, An Weiwei. Analysis on the Relationship between Shearing Force and Section Morphology of Sheet Shears [J]. Forging Equipment & Manufacturing Technology, 2021,56(1):88-90,99.

[11] Qiu Lin. Design and Research of High Speed Shearing machine frame based on ANSYS [J]. Journal of Liaoning University of Technology (Natural Science Edition), 2014, 34(2):103-106.

Viser Technology Pte. Ltd.
Mechanical Engineering Science
DOI: 10.33142/mes.v5i1.12713

Research Article Open Access

Simulation Analysis of Extrusion Process of Equilateral L-shaped Aluminum Profiles Based on Deform-3D

Guangchen XU*, **Wenwu ZHANG, Sisi CHEN, Mantong WANG**

Yingkou Institute of Technology, Yingkou, Liaoning, 115014, China

***Corresponding Author:** *Guangchen XU, E-mail: kanu012@163.com*

Abstract:
The extrusion deformation process of L-shaped aluminum profiles was numerically simulated using the finite element program Deform-3D. The simulation findings revealed that the deformation of the profiles was mostly caused by unequal material flow velocity, which resulted in the profiles bending. Determine the impact of extrusion parameters on the bending deformation of the profile after studying various parameters that may affect the material flow mode (hole position, extrusion speed).
Keywords: *Deform-3D; extrusion processing; bending*

1 Introduction

Extrusion processing is a vital technique in the metalworking industry. The metal is normally heated to the temperature of plastic formation during the extrusion process, and then various shapes of goods are extruded using extrusion molds. Because the material properties of aluminum alloys vary at high temperatures, the flow mode of the material varies, affecting the quality of extruded products. Aside from temperature, mold design, friction conditions, and product form all influence material flow patterns. As a result, the aluminum alloy extrusion process is extremely complex, and the majority of mold design processes are empirical in nature, relying entirely on the experience of mold workers to construct the trial mold. There is no effective formula or criterion for reference.

Numerous academics both domestically and internationally have made great strides in their studies of the extrusion process of aluminum profiles in recent years by using numerical simulation methods. FANG et al. [1] used Deform-3D software to perform numerical analysis on the extrusion of a typical industrial profile, and they investigated the effects of extrusion speed and working strip length on the material's temperature distribution, the profile's dimensional accuracy, surface quality, and extrusion pressure over the course of the extrusion process;JO et al. [2] conducted numerical simulations on the production process of 7003 aluminum alloy pipes and obtained the influence of billet preheating temperature, extrusion ratio, working strip length, and aluminum pipe wall thickness on extrusion pressure, maximum temperature of profiles, surface quality of profiles, and dimension accuracy of the profile.SuperForge was utilized by WU et al. [3] to investigate the metal flow that occurs during the extrusion of rectangular hollow aluminum tubes. The shape and size of the diversion hole as well as the path shape from the diversion hole's inlet to the working zone were found to be the main factors affecting the flatness of the end face of the extruded rectangular hollow tube by comparing the results; Yan Hong et al. [4] used numerical methods to analyze the extrusion process of angle aluminum profiles and combined neural networks and genetic algorithms to optimize the extrusion process parameters.Mooi et al.[5] employed the finite element method to simulate profile flow and mold deformation during extrusion. Imamura et al.[6] provided a simple design solution for a guide plate to assure uniformity in plastic flow velocity at the exit of the mold, addressing the problem of expanding extrusion when the breadth of the profile is greater than the diameter of the original embryo; Jo et al.[3] investigated the influence of welding length on extrusion pressure for pipe fittings with numerous hole molds, as well as the link between extrusion pressure and temperature variations; In order to improve the extrusion condition of products, Ulysse and Johnson[7] proposed applying mathematical models to forecast plastic flow properties such as changes in flow velocity at the departure of extrusion molds. The majority of the preceding research focus on the flow plastic analysis of the early embryo in the mold, with

Copyright © 2023 by author(s) and Viser Technology Pte. Ltd. This is an Open Access article distributed under the terms of the Creative Commons Attribution-NonCommercial 4.0 International License (http://creativecommons.org/licenses/by-nc/4.0/), permitting all non-commercial use, distribution, and reproduction in any medium, provided the original work is properly cited.
Received on April 7, 2023; Accepted on May 27, 2023

little examination of the impact of mold elastic deformation on product size [8-13].

This article investigates the extrusion process of equilateral L-shaped aluminum profiles, investigates the effects of mold design and extrusion parameters on extrusion forming characteristics during the extrusion process, and provides a theoretical foundation for improving the quality of profile extrusion forming.

2 Design of Extrusion Processing Process

2.1 Selection of extrusion molds

Create the appropriate model for simulation using Solidworks program and save it in STL format. Figures 1 and 2 demonstrate profiles and mold models created with the finite element simulation program DEFORM-3D for extrusion forming simulation analysis.

The mother mold used in this study is a pocket die, which has benefits for extrusion that traditional flat molds do not have. These benefits include: (1) simple control over material flow; (2) minimal direct impact of extrusion pressure on the mold, minimizing mold damage; and (3) the ability to form a pre-formed extrusion ingot at the pocket to improve extrusion processing precision.

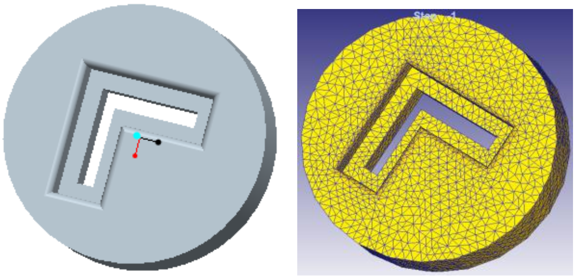

Figure 1 L-shaped profile diagram

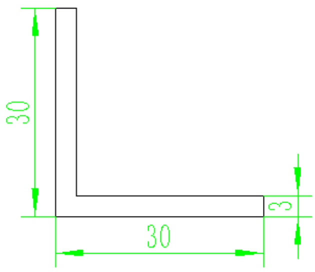

Figure 2 3D model and finite element model of pocket mold

2.2 Extrusion parameter setting

The secret to accurately simulating is to define boundary criteria. Because the extruded items in this study have a symmetrical shape, half of the models were chosen for examination and study. There is no deformation in the XZ and YZ planes of the DEFORM-3D finite element analysis because the extrusion direction is along the negative Z-axis direction. Consequently, the XZ and YZ planes' boundary conditions can be established by setting the displacement symmetric boundary to zero.

The simulation accuracy greatly depends on the calculation parameters that are established when the simulation analysis is initiated. Table 1 displays the primary extrusion simulation parameters based on the real extrusion production design.

Table 1 L-profile extrusion simulation parameters

Embryo Material (mm)	Embryo diameter (mm)	Number of Meshes	Extrusion Ratio	Extrusion Velocity (mm/s)	Outlet Velocity (mm/s)	Initial Temperature (°C)	Heat Transfer Coefficient (W/m°C)
100	80	30000	30	2.2	32	300	10

3 Simulation of Extrusion Processing

3.1 Analysis of defects in profile extrusion forming

Figure 3 depicts the extrusion flow rate diagram of an aluminum profile blank. The flow rate of the substance can be seen in Figure 3. The flow velocity in the middle of the profile is faster than the flow velocity on both sides, resulting in the first velocity difference; the flow velocity behind the profile is faster than the flow velocity in front of the profile, resulting in the second velocity difference. Because the two speed variations lead the billet to bend from a high flow rate area to a low flow rate area, uneven material flow rate is the primary source of bending errors in profile extrusion molding.

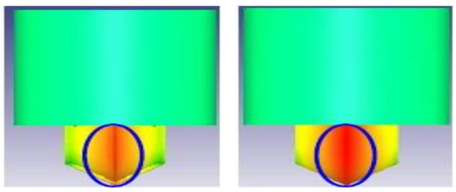

(a) Front view (b) Rear view

Figure 3 Flow velocity diagram of L-shaped profile billet

3.2 Analysis of mold hole position

Firstly, introduce the bending angle - β, Define the degree of deformation during extrusion and bending of profiles.

$$\beta=\langle\vec{A},\vec{B}\rangle=\cos^{-1}\frac{(A,B)}{|A||B|} \tag{3-1}$$

A and B are vectors representing two places on the mold outlet and profile, respectively. The ideal bending defect indicator value is zero, and the clockwise direction is positive; The greater this angle, the more severe the bending defect.

Examine how the location of the mold hole affects the profile extrusion forming's degree of bending. The locations of holes in L-shaped profiles are depicted in Figure 4. The origin (X=0) is defined as the position of the center on the symmetry axis, and the centroid position of the L-shaped profile hole in the figure is at the center of the circle. In order to mimic a total of five positions at the circle's center, the study approach involves choosing two locations in the positive X direction and two positions in the negative X direction. The centroid position of the L-shaped hole is displayed in Table 2. Figure 5 displays the flow velocity of the L-shaped profile blank at these five locations. The profile moves upward to its maximum when X = 8 mm, as Figure 5 illustrates; the profile moves downward to its maximum displacement when X =-12 mm. Furthermore, it was discovered through simulation that every profile had severe bending situations, and Figure 6 illustrates the bending situations of profiles at various centroid points. found using the graph β The angle is between 20° and 35 °, and the profile's bending is greatly affected by the hole's location.. Therefore, changing the position of the holes can effectively improve the bending defects in the extrusion forming of profiles.

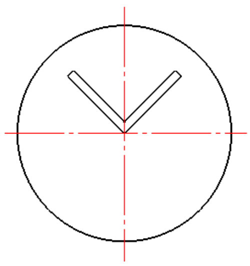

Figure 4 L-shaped profile hole location diagram

Table 2 Location of L-shaped hole centroid

location	1	2	3	4	5
X(mm)	8	4	0	-6	-12

(a)X=8 (b) X=4 (c) X=0 (d) X=-6 (e) X=-12

Figure 5 Flow velocity diagram of L-shaped profile billet

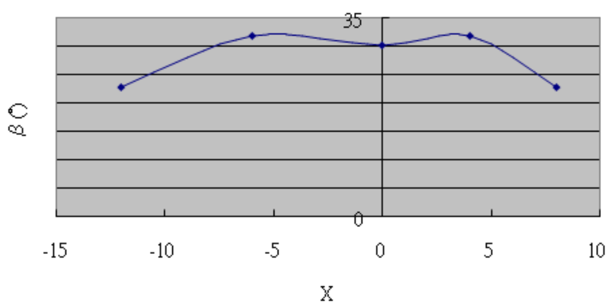

Figure 6 Bending trend of profiles at different centroid positions

Analyze the effect of extrusion speed on the bending degree of profile extrusion forming, and Figure 7 shows the bending situation of profiles at different extrusion speeds. As shown in the figure, the bending degree is most severe when the extrusion speed is 1.1mm/s. Table 3 shows the results under different extrusion speeds β The angle calculation results can be seen from the table β The angle decreases as the extrusion speed increases. Therefore, the bending degree of profile extrusion can be improved by changing the extrusion speed.

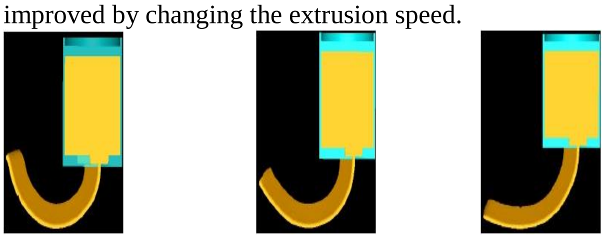

(a)v=1.1mm/s (b) v=2.2mm/s (c) v=3.4mm/s

Figure 7 Bending degree of profiles under different extrusion speeds

Table 3 Profile under Different Extrusion Speeds β horn

Extrusion Velocity(mm/s)	β(°)
1.1	30.2
2.2	23
3.4	18

4 Conclusion

In this work,two extrusion parameters—hole position and extrusion speed—are analyzed through simulation research on the extrusion process of L-shaped profiles.Through the use of bending indicators, the degree of extrusion bending deformation of profiles is assessed using the β Angle.The degree of bending of profiles is influenced by the position of the mold holes, and bending flaws can be efficiently rectified by repositioning the holes.The bending degree of the extruded profile can be enhanced by varying the extrusion speed,which can also affect the extrusion pressure.

Fund Project: The authors acknowledge the Natural Science Foundation of Liaoning (Grant: 2021-YKLH-03 2021-YKLH-04) and The 2023 Key scientific research project of Yingkou Institute of Technology (Grant: ZDIL202302).

References

[1]FANG G, ZHOU J, DUSZCZYK J.Extrusion of 7075 aluminium alloy through double-pocket dies to manufacture a complex profile [J]. Journal of Materials Processing Technology, 2009(209):3050-3059.

[2]JO H H, LEE S K, JUNG C S,et al.A non-steady state FE analysis of Al tubes hot extrusion by a porthole die[J]. Journal of

Materials Processing Technology, 2006, 173:223-231.
[3]WU X H, ZHAO G Q, LUAN Y G, et al. Numerical simulation and die structure optimization of an aluminum rectangular hollow pipe extrusion process [J]. Materials Science and Engineering A, 2006, 435-436:266-274.
[4]YAN Hong, XIA Juchen, HU Guoan.Optimization of technological parameters for profile extrusion process [J]. Chinese Journal of Mechanical Engineering, 2002, 38(10):78-81.
[5]H.G.Mooi, P.T.G.Koenis, J. Huetink.An Effective Split of Flow and Die Deformation Calculations of Aluminum Extrusion [J]. Journal of Materials Processing Technology, 1999(88):67-76.
[6]Y.Imamura,N.Takatsuji.Metal Flow Control by Flow Guide of Spreading Extrusion-Study of Spreading Extrusion Process-III[J]. Journal of the Japan Society for Plasticity of Technology, 1999(40):976-980.
[7]H.H. Jo, S.K. Lee, S.B. Lee.Prediction of welding pressure in the non-steady state porthole die extrusion of Al7003 tubes [J]. Journal of Materials Processing Technology, 1999(41):1067-1088.
[8]P.Ulysse.R.E. Johnson. A Die Design Model for Thin Section Extrusions [J]. International Journal of Mechanical Sciences, 1999(41):1067-1088.
[9]Wang Hai,Wang Zhongping. A New Processing Technology of Aluminum Profile without Rounded Corners of the Six Square Hole[J]. New Technology & New Process, 2015(3):15-17.
[10]Zhang Haichao.Study on Numerical Simulation of Extrusion Process, Die Optimization and Heat Treatment of Large Complex Aluminum Alloy Profile[D]. SHANDONG: SHANDONG University, 2023.
[11]Chen Hao, Zhao Guoqun, Zhang Cunsheng.Numerical Simulation of Extrusion Process and Die Structure Optimization for a Hollow Aluminum Profile with Thin Wall [J]. Journal of Mechanical Engineering, 2010(46):34-39.
[12]XU Zongtao, XIAO Chong.Research on the Machining Technology of Thin-Wall Aluminum Profile Parts for High-speed EMUs [J]. Modern Manufacturing Technology and Equipment, 2020, 56(1):140-141.

Viser Technology Pte. Ltd.
Mechanical Engineering Science
DOI: 10.33142/mes.v5i1.12714

Research Article Open Access

Study on Flow Field Optimization of Flow Distribution Disk of Double-unloaded Groove Piston Pump

Yuning SONG*

Yingkou Institute of Technology, Department of Mechanical and Power Engineering, Yingkou, Liaoning, 115014, China

***Corresponding Author:** *Yuning SONG, E-mail: songyuning1230@163.com*

Abstract:
By referring to all kinds of research data and summarizing the analysis and research of various kinds of distribution disks, a new type of distribution disc with double V-shaped unloading slots is designed again. Then, the new designed disk is loaded into the piston pump by CFD software to simulate. Finally, through simulation, it is concluded that the width of the triangle slot of the distribution plate is about 10 °, the slope angle is about 12 °, and the diameter of the unloading hole is about 0.8mm. When the diameter of the perforated hole is about 1.5mm, the flow curve of the unloading hole is the smoother. Pressure shock and noise are also minimized at this time. Draw By improving the damping tank, the flow noise and cavitation change are smaller than before.
Keywords: *Diskette; Double V discharge slot; CFD; Damping tank*

1 Introduction

According to the working principle of the axial piston pump and we know that in axial piston pump with flow table for interactive oil distribution, the valve plate plays an important role, with the hydraulic pump using the working reliability and life of great influence[1-3]. Pressure drop is too suddenly, the commonly used method is to open a small slot or hole to solve the impact phenomenon, make the oil pressure effect will not be too fierce, so as to resolve this sudden shock. Oil flow state and the axial plunger pump overall efficiency of performance are important [7-9].

Using three-dimensional modeling software SolidWorks on valve plate of 3 d modeling, and then use analytic software ANSYS in the process of its use is parsed, on its stress strain curve and deformation nephogram, through the finite element analysis software of the simulation results verify the valve plate can meet the requirements of actual working conditions.

2 Valve Disc Wear Mechanism

Plunger pump in the process of practical work, the workers often will not consciously to ignore in the valve plate with flow process of tiny pit phenomenon, but those tiny pit is caused by air pockets [10-12], under the research scholarsthat Na Chenglie research, he found the little bubbles will not only cause tremendous noise when burst, will flow on the plate cylinder piston cavity even cause pockmark. And also deduce the unit area of solid when the bubble burst, the specific algorithm can be calculated using the following formula of impulse to.

$$\mathrm{I} = \sqrt{2\mathrm{d}l\rho(p - \mathrm{p}_0)}$$

Type: p_0——The pressure of air pockets in the air;
l——Back into liquid liquid column length;
d——Raced back to the trip air bubble diameter;

Thus, when the bubble burst or annihilation, cylinder wall or with above all can form the cavitation flow plate or hemp pit phenomenon, this phenomenon with the diameter of the bubble, bubble pressure and the length of the plunger are closely linked. Therefore, the high pressure small diameter of cavity also cannot be ignored.

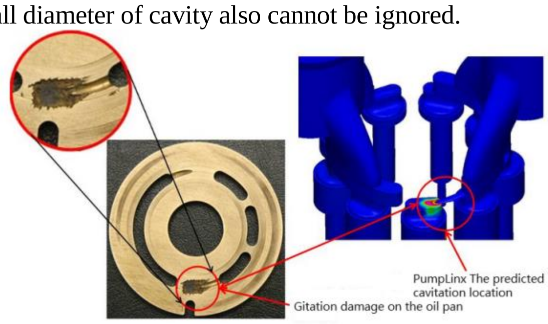

Figure 1 Validation of cavitation on the distribution plate

Copyright © 2023 by author(s) and Viser Technology Pte. Ltd. This is an Open Access article distributed under the terms of the Creative Commons Attribution-NonCommercial 4.0 International License (http://creativecommons.org/licenses/by-nc/4.0/), permitting all non-commercial use, distribution, and reproduction in any medium, provided the original work is properly cited.
Received on April 7, 2023; Accepted on May 19, 2023

3 Different Types of Buffer Unloading Trough Analysis

Commonly used at home and abroad with more flow plate type structure though, but the basic sum up about three, as shown in figure 2, the common characteristics are above the waist type slot open certain buffer structure. When people begin to design the valve plate and did not expect to be above the waist type slot to open any shape, the most to the left of the shape as shown in figure 2, this one people usually call them the new structure of tradition. But, this kind of valve plate in the use of plunger pump, plunger pump can produce a lot of noise, and one more thing is, the flow of oil outlet presents the pulsation phenomenon. As a result, people started to analyze what causes of noise and ripple, after analysis found that the oil from the low pressure mode in the process of transition to the tank high waist type slot, because there is no preset buffer tank, oil instead of buffer room directly into high pressure cavity of the high and low pressure chamber of the oil pressure differs very big, go directly to is bound to cause ripple and noise, so going to find a way to improve, thus was born the figure 2 of the other two types of surge tank, triangle groove or u-shaped slot. This two kinds of buffer tank with the accumulation of years basically deflection to the use of triangular groove. But the study found that the triangle groove opening, although can play a buffer role, but the tip of the triangle groove parts easy to form stress concentration phenomenon, in order to solve the problem of stress concentration, open small round hole in the top of the triangle groove to solve the problem of stress. This and formed a new type of surge tank, hole groove type. Although this kind of valve plate can play a buffer role, but also can not guarantee the working rotation to the high-pressure plunger slot when rise of pressure and rotation to the trough of leakage pressure are equal, or easy to cause cavitation.

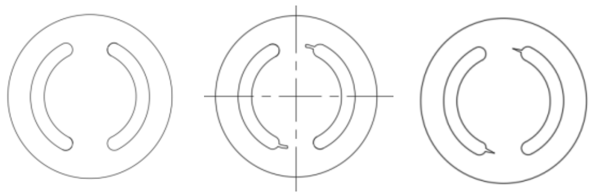

(a) (b) (c)

(a) Without damping groove

(b) U-shaped damping groove

(c) Triangle damping groove

Figure 2 The structure type of the buffer tank

But for the new structure of triangular groove is easy to produce cavitation and noise phenomenon, in bad reading a lot of information about the direction of the valve plate, decided to change my single triangle groove opening to double triangular groove, and under the damping hole to open oil duct, its structure as shown in figure as shown in 3.

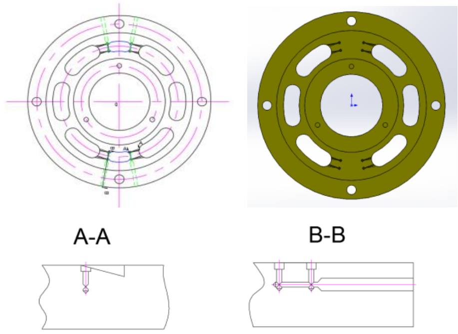

Figure3 Double buffered damping tank

4 Triangle Damping Groove Structure Design

In general, there must be a group in the actual work or combinations of several groups of data, makes the swashplate axial piston pump flow pressure in the process of impact on the smallest, minimum flow pulsation, the combination of minimum is noise data. However, due to such a complicated engineering problem, engineering practice and unable to provide detailed and accurate expression function, therefore, we once again on the basis of the original design, optimization design. The specific process as shown in figure 4:

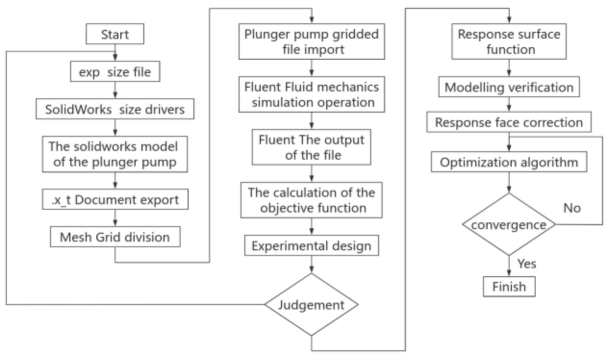

Figure 4 Buffer slot optimization design flow

5 Double Unloading Groove Plunger Pump with Flow Plate Flow Field Analysis

On the system of the internal flow field do certain simplified model, after I finish to simplify and according to the internal flow field of the actual operation situation made some basic assumptions, by assumption is as follows:

(1) Assuming that the hydraulic oil for incompressible fluid;

(2) Assume that the hydraulic oil for viscous Newtonian fluid;

(3) Assumes the flow field of the system is steady;

(4) Regardless of the fluid gravity;

(5) Assume that no heat transfer within the hydraulic oil;

(6) Even within the system with the gas, assumes that the continuity equation is still available.

If you want to mathematical modeling on the flow field in the system, you first need to understand what kind of software for simulation analysis system internal flows. The second is to understand how to establish the mathematical model of you need. In general, our internal flow field of the whole system with powerful fluid parse function parses the fluent software. According to the previous hypothesis conditions, system of internal flow field as a fixed flow field. For fixed field flow phenomenon, usually uses a continuous equation and Bernoulli Reynolds averaged navier-stokes equations. In the algorithm, usually uses a simple algorithm and PISO algorithm. Here, we give a k - epsilon model equations of tensor form;

$$\frac{\partial \rho}{\partial t}+\frac{\partial}{\partial x_i}(\rho u_i)=0 \tag{1}$$

$$\frac{\partial}{\partial t}(\overline{\rho u_i})+\frac{\partial}{\partial x_j}(\overline{\rho u_i u_j})=-\frac{\partial p}{\partial x_i}+\frac{\partial}{\partial x_j}(\mu\frac{\partial u_i}{\partial x_j}-\rho \overline{u_i^{'} u_j^{'}})+S_i \tag{2}$$

$$\frac{\partial}{\partial t}(\rho k)\frac{\partial}{\partial x_i}(\rho k u_i)=\frac{\partial}{\partial x_j}((\mu+\frac{\mu_t}{\sigma k})\frac{\partial k}{\partial x_j})+G_k+G_b-\rho\varepsilon-Y_M+S_k \tag{3}$$

$$\frac{\partial}{\partial t}(\rho\varepsilon)+\frac{\partial}{\partial x_i}(\rho\overline{\varepsilon u_i})=\frac{\partial}{\partial x_j}((\mu+\frac{\mu_t}{\sigma_k})\frac{\partial \varepsilon}{\partial x_j})+C_{1\varepsilon}\frac{\varepsilon}{k}(G_k+G_{3\varepsilon}G_b)-G_{2\varepsilon}\rho\frac{\varepsilon^2}{k}+S_\varepsilon \tag{4}$$

Type (1) as the continuity equation, the pattern is too all forms of Reynolds equation (2), type (3) the transport equation of turbulent kinetic energy k and epsilon type (4) is the turbulent kinetic energy dissipation rate of the transport equation.

Reynolds stress:

$$-\rho\overline{u_i^{'} u_j^{'}}=\mu_t(\frac{\partial u_i}{\partial x_j}+\frac{\partial u_j}{\partial x_i})-\frac{2}{3}(\rho k+\mu_i\frac{\partial u_i}{\partial x_j})\delta_{ij}$$

, Among them: μ_t is the turbulent kinetic energy, $\mu_t=\rho C_\mu\frac{k^2}{\varepsilon}$;

u_i is the average speed per hour;

δ_{ij} is the Kronecker delta;

k is the urbulent kinetic energy, $k=\frac{\overline{u_i u_i}}{2}=\frac{1}{2}(u'^2+v'^2+w'^2)$;

$u_i{}'$ is the fluctuating value;

ε is the turbulent dissipation rate, $\varepsilon=\frac{\mu}{\rho}\overline{(\frac{\partial u_i^{'}}{\partial x_k^{'}})(\frac{\partial u_i^{'}}{\partial x_k^{'}})}$;

G_k is the due to the change of gradient generation rate, resulting in the turbulent kinetic energy k, $G_k=\mu_t(\frac{\partial u_i}{\partial x_j}+\frac{\partial u_j}{\partial x_i})\frac{\partial u_i}{\partial x_j}$.

G_b is caused by the buoyancy of turbulent kinetic energy k, for incompressible fluids, G_b=0; forcompressiblefluids, $G_b=\beta g_i\frac{\mu_t}{\Pr_t}\frac{\partial T}{\partial x_i}$;

β is the thermal expansion coefficient, $\beta=-\frac{1}{\rho}\frac{\partial\rho}{\partial T}$;

P_{rt} is turbulent Prandtl number, in general, P_{rt}=0.85, g_i is the gravitational acceleration in the direction of the ith component.

Y_M representatives can be compressed fluctuations in the turbulent diffusion effect. For incompressible fluids, Y_M=0; For compressible fluids, $Y_M=2\rho\varepsilon M_t^2$, M_t is turbulent Mach number, $M_t=\sqrt{\frac{k}{a^2}}=\sqrt{\frac{k}{\gamma RT}}$.

Table1 High-pressure axial piston pump geometric model of the parameters

Parameter	Numerical	Parameter	Numerical
Pump Displacement Q	66cm^3/R	Distribution Of Plug Diameter D	77mm
The Maximum Load Pressure P	35mp	Adjacent Piston Angle Θ_0	40°
Cylinder Speed N	1500r/Min	The Plunger Hole Angle Range Ψ_0	25°
Plunger Number Z	Nine	The Initial Length Of Closed Volume L_0	22.1mm
Plunger Diameter D	19mm	Swash Plate Angle A	16°

$C_{1\varepsilon}$, $C_{2\varepsilon}$, $C_{3\varepsilon}$is empirical constan, σ_k and σ_εAnd the turbulent kinetic energy K and dissipation rate ε corresponding Prandtl number, S_i、S_k、$S_{\varepsilon i}$ is user defined the source term. In the standard k - epsilon model, they respectively values as follows: $C_{1\varepsilon}$=1.44; $C_{2\varepsilon}$=1.92; C_μ=0.09; σ_k=1.0; σ_ε=1.3; For $C_{3\varepsilon}$, in compressible fluid, when the main flow direction and the gravity direction is parallel to each other, $C_{3\varepsilon}$=1, Similarly, when they are perpendicular, $C_{3\varepsilon}$=0.

Set up the new structure of four kinds of structure forms, respectively with traditional flow plate, with the new structure of V groove, the new structure of with u-shaped slot, and the new structure of double V groove.

Will be the new structure of four different structure forms, respectively with full port model (as shown in figure 5, figure 6) of the other components are combined, and then to compile analysis respectively, and the real-time monitoring for the export of oil, get export the flow curve of the oil, because did not take into account the oil leakage in the process of simulation, so it can monitor the flow of imported oil pump. Due to the different shape structure formed by the valve plate looks similar to the velocity field and pressure field distribution of change trend is basically the same. The difference is the size of the pressure value and speed.

In the process of practical work, each rotary plunger can produce 2 z flow pulsation in a week. Popular speaking, when a plunger cavity filled with oil absorption in the waist with the valve plate type when connected to oil tank, oil discharge cavity of the actual working pressure generally higher plunger cavity oil pressure at this time, the poor and large load pressure). At this point, the discharge of oil waist type high pressure oil instantaneous slot will pressure into the plunger cavity, not only that, this part is instantaneous pressure into the plunger cavity of high pressure oil will flow through the flow pulsation in suction tank, this case the flow pulsation values are higher than the conventional pulse value of cases in other circumstances. Valve plate of oil outlet flow curve as shown in figure 11-14.

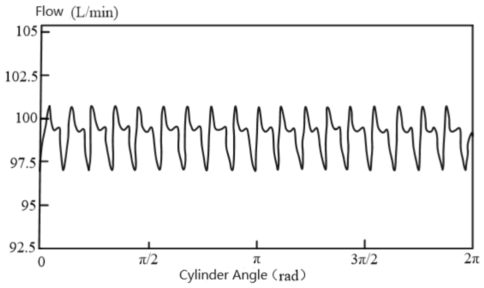

Figure 11 Flow curve of traditional distribution plate

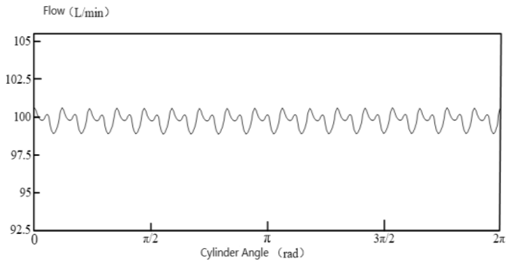

Figure 12 Variation curve of U-slot platen

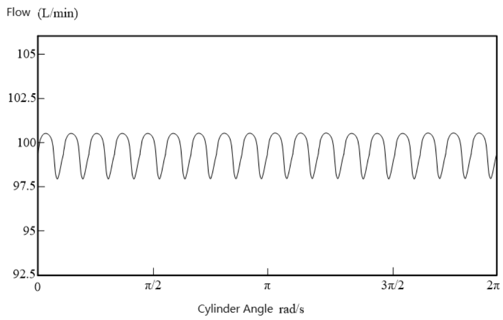

Figure 13 Variation curve of V-slot platen

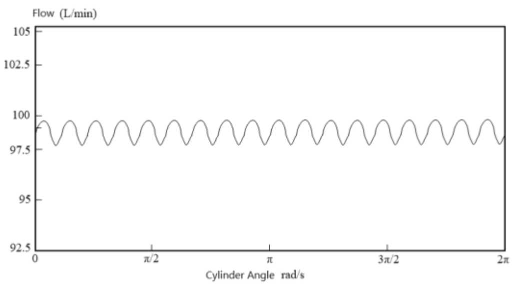

Figure 14 Double V-groove distribution plate change curve

Table 2 Flow pulsation of different shapes of the dispensing tray model

Model	Q_{max} L/Min	Q_{min} L/Min	Q_{ave} L/Min	Δ %
Traditional	100.83	96.89	98.86	3.99
Single U	100.72	97.36	98.875	3.34
Single V	100.56	97.96	99.31	2.62
Double V	100.48	98.84	99.56	1.65

Through the analysis of 11-14, valve plate to join don't open any damping groove of flow fluctuation is bigger, and excessive is not smooth, a sharp peak, this situation is not conducive to the stability of pump, and because the peak is basically straight on straight down, cause the noise of the impact is bigger. Observed from figure 4.7 in turn down 4.10 can be found that the new structure of open u-shaped damping groove in the flow curve has slowed, but also in reducing volatility, but we want to make impact become smaller, to connect with flow plate and plunger cavity, smooth flow pulsation is becoming as much as possible, floating values become as small as possible, to reduce the noise, shock, we have designed the new structure of double "V" damping groove, on the one hand, V groove pointed mouth place from high pressure oil, can reduce half of the impact of noise can be reduced, and by observing the graph can be flow pulsation became more and more small, you may refer to specific parameter values are shown in table 2. Simulation proves that this design is helpful to improve the work efficiency of the pump noise, reduce the flow pulsation.

6 Process and Results Optimized by Using the Penalized Function Method

The span a and the width b of the triangle groove are defined as the design factors, the span of the high pressure side buffer groove of the distribution plate is recorded as a1 width as b1, the span of the low pressure side buffer groove is recorded as a2 width as b2, and the full factor method is used to obtain some arrangement and combination of the two factors. So-called full factor analysis is actually each factor in the experiment in accordance with the combination of combination results minus 1, combination of all factors are participated in not less than two independent repeated experiment, we put the formation of the full arrangement combination of new experimental factor method called full factor method. For example, factors m1, m2, m3, m4 combined 2k-1 (k =4), then we need to do 15 trials, in which the main effect is m1, m2, m3, m4, and the interaction effect is m 1 m 1, m1m3, m1m4, m2m3, m3m4, m1m2m3, m1m2m4, m2m3m4, m1m2m3m4, a total of 15 experiments.

In the test process, in order to avoid the problems of large calculation amount and low efficiency in the redesign process, the second-order response surface function is generally selected as the target performance approximate model of the inclined disc axial plunger pump, as shown in Equation 5.

$$F = a_0 + \sum_{i=1}^{n} a_i X_i + \sum_{i=1}^{n}\sum_{j=1}^{n} b_{ij} X_i X_j \tag{5}$$

According to the structural characteristics of the pump and the processing and installation requirements, the width of the groove, a1, b1, a2, and the width of the damping groove are a11, a12, a 12, a13, a14, with a width, b11, b12, b13, and a21, a22, b22, b23, b24, as shown in Es. 6.

$$\begin{cases} 0 \le a_{11} \le 20° \\ 0 \le b_{11} \le 5 \\ 0 \le a_{21} \le 20° \\ 0 \le b_{21} \le 5 \end{cases}, \begin{cases} 0 \le a_{12} \le 20° \\ 0 \le b_{12} \le 5 \\ 0 \le a_{22} \le 20° \\ 0 \le b_{22} \le 5 \end{cases}, \begin{cases} 0 \le a_{13} \le 20° \\ 0 \le b_{13} \le 5 \\ 0 \le a_{23} \le 20° \\ 0 \le b_{23} \le 5 \end{cases}, \begin{cases} 0 \le a_{14} \le 20° \\ 0 \le b_{14} \le 5 \\ 0 \le a_{24} \le 20° \\ 0 \le b_{24} \le 5 \end{cases} \tag{6}$$

In order to use the constraint function expression, the optimization variable, the span angle a1, the low-voltage damping groove width b1, the angle a2, and the high-pressure damping groove width b2 are expressed as constraint functions, as shown in Equation 7.

$$\begin{cases} g_1(X) = -x_1 \le 0, \; g_2(X) = 20 - x_1 \le 0 \\ g_3(X) = -x_2 \le 0, \; g_4(X) = 5.0 - x_2 \le 0 \\ g_5(X) = -x_1' \le 0, \; g_6(X) = 20 - x_1' \le 0 \\ g_7(X) = -x_2' \le 0, \; g_8(X) = 5.0 - x_2' \le 0 \end{cases} \tag{7}$$

The theoretical expression of the objective performance is shown in Equation 8,9 and 10.

$$\begin{cases} \Delta P_H = 10^{-3} \cdot \left[-0.108x_1^2 - 0.814x_2^2 - 12.455x_1 \cdot x_2 + 148.800x_1 + 5.914x_2 - 876.252\right] \\ Q_h = 10^{-3} \cdot \left[0.0896x_1^2 + 2.132x_2^2 - 13.81x_1x_2 - 9.633x_1 + 55.039x_2 + 197.98\right] \end{cases} \tag{8}$$

$$\begin{cases} \Delta P_L = 10^{-3} \cdot \left[-2.2x_1'^2 - 1.8x_2'^2 + 1.8x_1' \cdot x_2'^2 + 73.2x_1' - 66.7x_2' - 618.8\right] \\ Q_l = 10^{-3} \cdot \left[20.0x_1'^2 - 24.1x_2'^2 + 10.4x_1' \cdot x_2' - 130.3x_1' + 188.3x_2' - 372.1\right] \end{cases} \tag{9}$$

$$R^2 = 1 - \frac{\sum_{j=1}^{N}[y_{rsm}(j) - y(j)]^2}{\sum_{j=1}^{N}[y(j) - \bar{y}]^2} \tag{10}$$

Formula: it is the difference between the maximum pressure and the minimum pressure in the inner chamber with high pressure; Qh refers to the flow flow in the simulation true value and the plane response value of the planned size; represents the simulation mean of each point in the design space; N represents the number of test points in the design space. R2 represents the determination coefficient, and the size of its value represents the difference between the reaction plane and the simulation plane value. If the value is within 0-1, when the value is 1, it means that the two are basically the same.

The function expression can basically reflect the performance of the objective function about the response of local structural changes, which can further replace CFD simulation, and finally optimize and redesign the objective function, so as to improve the design efficiency of integration. Through the construction of the model and the CFD simulation test, the target performance function can be obtained, because there is a difference between the maximum value of inversion and pressure difference, so we introduce a new coefficient sum, so that the optimization values F1 and F2 of the overall structural design scheme can be obtained.

$$F_1 = \Delta P_H + \lambda_1 Q_H \tag{11}$$

$$F_2 = \Delta P_L + \lambda_2 Q_1 \tag{12}$$

among:

$$\lambda_1 = \frac{(\Delta P_H)_{\max} - (\Delta P_H)_{\min}}{(Q_H)_{\max} - (Q_H)_{\min}} \tag{13}$$

$$\lambda_2 = \frac{(\Delta P_L)_{\max} - (\Delta P_L)_{\min}}{(Q_L)_{\max} - (Q_L)_{\min}} \tag{14}$$

Here we choose the penalized function algorithm, and adopt the sorting method to solve the minimum value in Matlab. The design results are shown in Table 3.

Table 3 Optimized results for manifolds

Optimize the variable	Buffer tank structure in the low-pressure zone								High-pressure zone buffer groove structure							
	a_{11}	a_{12}	a_{13}	a_{14}	b_{11}	b_{12}	b_{13}	b_{14}	a_{21}	a_{22}	a_{23}	a_{24}	b_{21}	b_{22}	b_{23}	b_{24}
Before optimization	10				3		3		10				3		3	
postoptimality	9.884				3.532		3.332		11.365				2.561		2.31	

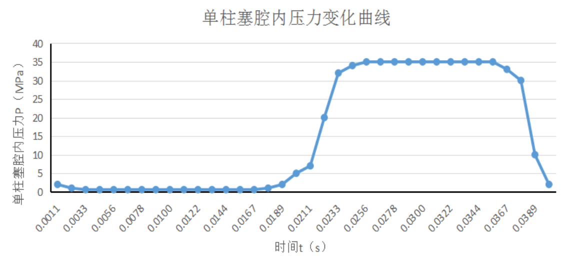

(a) Pressure change curve in a single plunger chamber

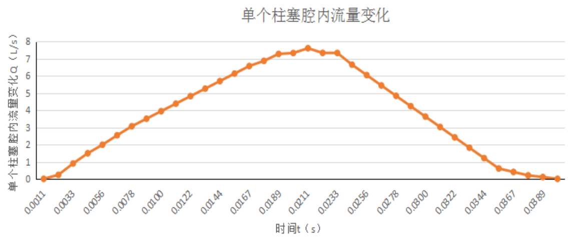

(b) Flow change curve in a single plunger cavity

Figure 15 Damping groove optimization design cavity after the curves of pressure flow curve

The optimized triangle groove was modeled in 3 D with SolidWorks, and Fluent software was used to simulate the relationship between pressure and flow in the plunger cavity. The simulation results are shown in Figure 15.

7 Conclusion

Through simulation with flow plate of triangle groove width open width is 10 ° or so, the best slope Angle is about 12 °, the unloading hole at about 0.8 mm in diameter of holes, the unloading hole punched at about 1.5 mm in diameter of flow curve when compared with the smooth. At the same time, the impact pressure and noise also is the smallest. Is obtained by the improvement of damping groove, traffic noise and cavitation are becoming smaller than before.

Fund project: The Regional Joint Foundation plan of the Provincial Natural Science Foundation in 2022“Study on the characteristics of hydraulic frequency conversion vibrator for rotary valve distribution”(2022-YKLH-07);The Basic Scientific research Project of the Provincial Department of Education in 2023“Analysis of voltage control characteristics and transient temperature of electro-hydraulic transmission”(JYTMS20230063).

References

[1] Huang Hai-nan, He Xue-ming. Desalination in axial piston pump with flow plate structure optimization [J]. Pump Technology, 2018 (1):10-15.

[2] Kong Xiang-chun, Nie Song-lin, Yin Fang-long. Water finale to the vibration characteristics of the plunger pump with flow are studied [J]. Hydraulics Pneumatics & Seals, 2018, 38(4): 28-32.

[3] Chi Yu-rong, Yang Jun-ru. Simulation and Research on Flow Pulsation of Axial Piston Pump [J]. Machine Tool ＆ Hydraulics, 2018, 46 (13): 138-143.

[4] Hao Xi-yang, Wang Yu-lin. Study on Damping Groove Characteristics of Axial Plunger Pump [J]. Agricultral Equipment & Vehicle engineering, 2018, 56(7): 48-51.

[5] Hou Wei, Nei Song-lin, Yin Fang-long. Optimization and Experimental Research for Silencing Groove Structure of Valve Plate in Water Hydraulic Piston Pump [J]. Chinese Hydraulics & Pneumatics, 2017 (8):8-13.

[6] Diao Ying-xi. Four match flow axial piston pump with flow characteristic analysis and research [D]. Taiyuan technology university , 2017.

[7] Cheng Jie. Axial piston motor with four match flow window flow theory and characteristic research [D]. Taiyuan university of science and technology, 2017.

[8] Chi Yu-rong. The axial plunger pump output flow pulsation and the dynamic characteristics of the research [D]. Shandong university of science and technology, 2017.

[9] Shi Xiang, Zhao Dong-biao. Structure Optimization of the Valve Plate of Aviation Piston Pump [J]. Machine Tool ＆ Hydraulics, 2015, 43(22): 57-60.

[10] ZAHANG Yi, Gao You-shan. Simulation and Analysis of Axial Piston Pump with Four Distribition Windows [J]. Hydraulics Pneumatics & Seals, 2016, 3 6(3):18-21.

[11] Shi Yan-ping, Zhang Yi. Simulation on Application of Axial Piston Pump with Parallel Dual Sucking and Discharging [J]. Hydraulics Pneumatics & Seals, 2016, 36(6):33-37.

[12] Shi Ying-xun, Meng Guang-yao. Simulation Study on Effects of the Shape of Damping Groove on Cavitating Flow [J]. Chinese Hydraulics & Pneumatics, 2016(8): 108-111.

[13] Chen Shuang-cheng. Based on the CFD desalination key techniques of axial piston pump [D]. Jiangnan university, 2016.

[14] Yin Jin-feng. The structure of the axial piston pump damping groove optimization design [D]. Henan university of science and technology, 2015.

[15] Bing XU, Ying-hui SUN, Jun-hui ZHANG, et al.. A New Design method for the transition Zone of Axial Piston pump Disc [J]. Journal of Zhejiang University-Science A(Applied Physics & Engineering), 2015,16(3):229-240.

Viser Technology Pte. Ltd.
Mechanical Engineering Science
DOI: 10.33142/mes.v5i1.12715

Research Article Open Access

Design of High Precision CNC Vertical Lathe Turning Tool Holder

Wenwu ZHANG, Guangchen XU, Lin QIAN, Mantong WANG*

Yingkou Institute of Technology, Yingkou, Liaoning, 115000, China

***Corresponding Author:** *Jiayu LI, E-mail: 13509779@qq.com*

Abstract:
A large aspect ratio vibration reducing tool holder based on passive damping vibration reduction technology is designed to solve the vibration problem that occurs in deep hole machining of vertical lathes.A dynamic model of passive damping vibration reduction tool holder was established, and the optimal damping ratio, optimal frequency ratio, and maximum relative amplitude were derived. Modal analysis of the passive damping vibration reduction tool holder was conducted using software.The results showed that the maximum response amplitude of the passive damping vibration reduction tool holder decreased significantly compared to the original one.
Keywords: *CNC vertical lathe; Cutting chatter; Cutting tool holder*

1 Introduction

Mechanical manufacturing is an important industry in today's society and a pillar industry for China's economic development, social progress, and national defense industry. The accuracy, efficiency, quality, and economy of mechanical processing are intuitive manifestations of the level of national manufacturing industry.

Since the 20th century, China has gradually become a major manufacturing country and a world OEM factory. However, there is still a significant gap in the overall level of high-end manufacturing between China and countries such as Europe and America. The gap between manufacturing powers and manufacturing powers is a challenge that we need to overcome. The reason for this dilemma is the gap in mechanical manufacturing equipment in China. With the continuous development of mechanical manufacturing equipment, the requirements for high-precision machining level and precision machining technology in mechanical processing are constantly increasing.

Among the overall stiffness of CNC vertical lathes, the vertical tool holder has the lowest stiffness, with large cutting volume or vertical ram extension length, which can cause vibration during machining, leading to a decrease in workpiece machining accuracy, reduced surface smoothness, and even tool breakage. This project is based on the design of the VCT16-NC CNC vertical lathe turning tool holder. On this basis, a dynamic model of the damping dynamic damping slider is established, and the damping dynamic damping technology is used to analyze the damping dynamic damping of the VCT16-NC CNC vertical lathe turning tool holder.Using anti vibration theory, improve the cutting stiffness of the vertical tool holder, and achieve a length to diameter ratio (the ratio of the extended length of the slider to the interface edge length of the slider) greater than "5" or greater under the maximum cutting force state of the slider without generating cutting chatter.To achieve many advantages such as improving machining accuracy, surface smoothness, seismic resistance, and machining efficiency, if the research results of this project are promoted and used in the machine tool industry, economic and social benefits will be obtained.

In recent years, domestic and foreign scholars have conducted extensive research on machining chatter, and have recognized that taking certain measures to reduce or eliminate tool vibration is an important method to ensure machining quality. At present, the main directions for applying damping and vibration reduction include the damping system of Taipei 101 Building, the damping and vibration reduction boring bar of Swedish Sandvik Company, and the damping system applied in the high-speed rail field. We take the damping and vibration reduction boring bar of Swedish Sandvik Company as the research object to complete the vibration reduction design of the turning tool holder.

Cutting chatter is a mechanical vibration generated during the machining process, which can affect the accuracy and surface roughness of the workpiece,

Copyright © 2023 by author(s) and Viser Technology Pte. Ltd. This is an Open Access article distributed under the terms of the Creative Commons Attribution-NonCommercial 4.0 International License (http://creativecommons.org/licenses/by-nc/4.0/), permitting all non-commercial use, distribution, and reproduction in any medium, provided the original work is properly cited.
Received on April 7, 2023; Accepted on May 22, 2023

accelerate the wear of machine tools, and reduce production efficiency. During the machining process, cutting chatter is inevitable, and the tool rest ram is the weakest part of the lathe tool rest in terms of stiffness. During the production process, the larger the aspect ratio of the tool rest ram, the lower its stiffness, and the easier it is to generate cutting chatter. To reduce the impact of cutting chatter on machining, a damping damper is placed in the inner cavity of the tool rest ram, By damping the relative vibration between the shock absorber and the knife rest ram, the kinetic energy of the knife rest ram vibration is consumed, thereby achieving the effect of vibration reduction.

2 Theoretical Model Establishment of Vibration Damping Ram

2.1 Structural design of damping dynamic damping ram

The damping dynamic damping ram consists of two parts: a knife rest ram and a damping system, where the damping system consists of damping fluid, damping blocks, and circular rubber rings. The damping fluid surrounds between the damping block and the annular rubber ring, providing resistance to the movement of the damping block. The damping block in the damping system is used as a "vibration core" throughout the entire ram. According to the theory of vibration absorbers, the heavier the mass block, the more obvious the damping effect. Therefore, the vibration core material is high-density hard alloy. The annular rubber ring is installed at both ends of the damping block as a support component to provide support for the damping block, ensuring that there is no contact or elastic collision between the damping block and the ram. The annular rubber ring has a high elastic modulus, and within its elastic range, the radial deformation of the annular rubber ring can provide a certain spring stiffness for the damping block, and has a certain linear relationship with the load it is subjected to. During the machining process, the ram is subjected to impact loads, resulting in cutting chatter. The internal vibration core generates forced vibration, and the damping system begins to work, absorbing the kinetic energy of the ram vibration, thereby playing a role in vibration reduction.

2.2 Simplified model of damping ram

The force analysis of the original model of the ram can be divided into two types: radial force and torque. The position of the ram near the tool holder is analyzed, and the influence of torque on the model is relatively small. It is ignored here. In the process of studying the damping ram, an equivalent substitution method is used to select the center position of the damping block as the research object, and the mass of the damping block is equivalent in this regard, Equivalent the mass of the ram to a mass block acting on the point we are studying, and equivalent the spring stiffness provided by the annular rubber ring to the equivalent elastic coefficient at the research point. Establish a dynamic model of the damping ram:

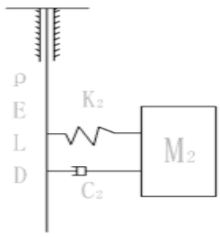

Figure 1 Original model of the ram

ρ—Material density of the ram; E—Elastic modulus of ram material;L—The elongation length of the ram during operation;K—Equivalent spring stiffness at the research point;K_1—Equivalent stiffness coefficient of annular rubber ring;D—Dimensions of the ram interface;C_2—Damping coefficient of ram damping fluid;M_2—Mass of damping block

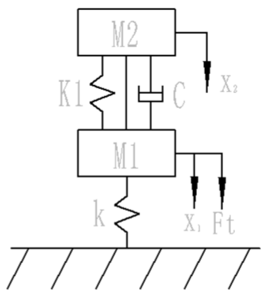

Figure 2 Dynamic model of damping ram

For the convenience of our research, we found that the motion mode of the damping ram is the same as that of the damping boring bar. Therefore, we equivalent the damping ram to an enlarged damping boring bar. Due to the complexity of the dynamic calculation of the damping ram, we use the formula in [1] to calculate it. We assume that only one impact load $F_{(t)} = Fe^{i\omega t}$ acts on M1 and establish the following equation based on Newton's second law:

$$\begin{cases} M_1\ddot{X}_1 + c\left(\dot{X}_1 - \dot{X}_2\right) + K_1\left(X_1 - X_2\right) + KX_2 = F_{(t)} \\ M_2\ddot{X}_2 - c\left(\dot{X}_1 - \dot{X}_2\right) - K_1\left(X_1 - X_2\right) = 0 \end{cases} \quad (1)$$

Solved:

$$\begin{cases} x_1 = B_1 \exp\left[i\left(\omega t - \varphi_1\right)\right] \\ x_1 = B_2 \exp\left[i\left(\omega t - \varphi_2\right)\right] \end{cases} \quad (2)$$

The first and second derivatives are:

$$\begin{cases} \dot{x}_1 = iB_1\omega \exp\left[i\left(\omega t - \varphi_1\right)\right] \\ \ddot{x}_1 = -B_1\omega^2 \exp\left[i\left(\omega t - \varphi_1\right)\right] \end{cases} \quad (3)$$

$$\begin{cases} \dot{x}_2 = iB_2\omega \exp\left[i\left(\omega t-\varphi_2\right)\right] \\ \ddot{x}_2 = -B_2\omega^2 \exp\left[i\left(\omega t-\varphi_2\right)\right] \end{cases} \tag{4}$$

Substitute its first and second derivatives into equation system:

$$\left.\begin{aligned} &\left[k+k_1-M_1\omega^2+i\omega c\right]B_1\exp\left[i\left(\omega t-\varphi_1\right)\right]-\left(k_1+i\omega c\right)B_2 xp\left[i\left(\omega t-\varphi_2\right)\right]=F\exp\left(i\omega t\right) \\ &\left[k_1-M_2\omega^2+i\omega c\right]B_2\exp\left[i\left(\omega t-\varphi_2\right)\right]-\left(k_1+i\omega c\right)B_1 xp\left[i\left(\omega t-\varphi_1\right)\right]=0 \end{aligned}\right\} \tag{5}$$

Expressed in matrix form as:

$$\begin{pmatrix} k+k_1-m_1\omega^2+i\omega c & -\left(k_1+i\omega c\right) \\ -\left(k_1+i\omega c\right) & k_1-m_1\omega^2+i\omega c \end{pmatrix}\begin{Bmatrix} B_1\exp\left(-i\varphi_1\right) \\ B_2\exp\left(-i\varphi_2\right) \end{Bmatrix}=\begin{Bmatrix} F \\ 0 \end{Bmatrix} \tag{6}$$

The amplitude expression is: $k = m\omega_n^2 = 23886.8\ N/mm$

Obtain:

$$\begin{cases} B_1\exp\left(-i\varphi_1\right)=\dfrac{\left(k_1-m_1\omega^2+i\omega c\right)F}{\left(k+k_1-m_1\omega^2+i\omega c\right)\left(k_1-m_2\omega^2+i\omega c\right)-\left(k_1+i\omega c\right)^2} \\ B_2\exp\left(-i\varphi_2\right)=\dfrac{\left(k_1+i\omega c\right)F}{\left(k+k_1-m_1\omega^2+i\omega c\right)\left(k_1-m_2\omega^2+i\omega c\right)-\left(k_1+i\omega c\right)^2} \end{cases} \tag{7}$$

Solve out B_1, B_2, expression:

$$\begin{cases} B_1=\dfrac{F\sqrt{\left(k_1-\omega^2 m_2\right)^2+\left(\omega c\right)^2}}{\sqrt{\left[\left(k-\omega^2 m_1\right)\left(k_1-\omega^2 m_2\right)-\omega^2 m_2 k_1\right]^2+\left[\left(\omega c\right)\left(k-\omega^2 m_1-\omega^2 m_2\right)\right]^2}} \\ B_2=\dfrac{F\sqrt{\left(k_1\right)^2+\left(\omega c\right)^2}}{\sqrt{\left[\left(k-\omega^2 m_1\right)\left(k_2-\omega^2 m_2\right)-\omega^2 m_2 k_1\right]^2+\left[\left(\omega c\right)\left(k-\omega^2 m_1-\omega^2 m_2\right)\right]^2}} \end{cases} \tag{8}$$

$$\left(\frac{B_1}{\delta_{st}}\right)^2=\frac{\left(a^2-\lambda^2\right)^2+\left(2\xi\alpha\lambda\right)^2}{\left[\left(1-\lambda^2\right)\left(a^2-\lambda^2\right)-\mu\lambda^2 a^2\right]^2-\left(2\xi\alpha\lambda\right)^2\left(1-\lambda^2-\mu\lambda^2\right)^2} \tag{9}$$

$$\left(\frac{B_2}{\delta_{st}}\right)^2=\frac{\alpha^4+\left(2\xi\alpha\lambda\right)^2}{\left[\left(1-\lambda^2\right)\left(a^2-\lambda^2\right)-\mu\lambda^2 a^2\right]^2+\left(2\xi\alpha\lambda\right)^2\left(1-\lambda^2-\mu\lambda^2\right)^2} \tag{10}$$

Do variable substitution:

$$\omega_{n1}=\sqrt{\frac{K}{M_1}},\quad \omega_{n2}=\sqrt{\frac{K_1}{M_2}},\quad \mu=\frac{M_2}{M_1},\quad \alpha=\frac{\omega_{n2}}{\omega_{n1}},\quad \xi=\frac{c}{2\sqrt{m_2 K_1}},$$

$$\lambda=\frac{\omega}{\omega_{n1}},\quad x_{st}=\frac{Fe^{i\omega t}}{K} \tag{11}$$

The relative displacement expression of the replaced damping ram:

$$S=\sqrt{\frac{\left(\alpha^2-\lambda^2\right)^2+4\alpha^2\xi^2\lambda^2}{\left[\left(1-\lambda^2\right)\left(\alpha^2-\lambda^2\right)-\mu\alpha^2\lambda^2\right]^2+4\alpha^2\xi^2\lambda^2\left(1-\lambda^2-\mu\lambda^2\right)^2}} \tag{12}$$

2.3 Relative displacement and frequency curve of damping ram

In the function of S about α, μ, λand ξ, using ξ as a variable, order α=0.916, order μ=0.0915.Draw the relative amplitude to frequency ratio curve of the damping ram in MATLAB software:

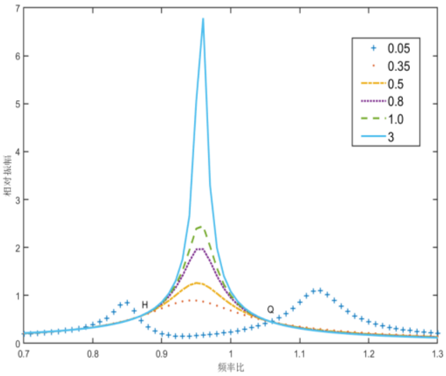

Figure 3 Curve of relative displacement to frequency ratio

In the figure, we can see that the curves of curve a under different damping conditions intersect at two points b and c.Regardless of the damping value, the relative displacement to frequency ratio curve passes through H and K.Therefore, the properties of these two points are independent of the magnitude of the damping ratio.Substituting a=0 and b=∞ into function S respectively yields:

$$\begin{cases} S_0=\dfrac{\left(\alpha^2-\lambda^2\right)}{\left(1-\lambda^2\right)\left(\alpha^2-\lambda^2\right)-\mu\alpha^2\lambda^2} \\ S_\infty=\dfrac{1}{\left(1-\lambda^2-\mu\lambda^2\right)} \end{cases} \tag{13}$$

The intersection point of the S_0 and S_∞ amplitude curves, namely the H and K points. Due to the opposite response of and, there are:

$$\frac{\alpha^2-\lambda^2}{\left(1-\lambda^2\right)\left(\alpha^2-\lambda^2\right)-\mu\alpha^2\lambda^2}=\frac{-1}{\left(1-\lambda^2-\mu\lambda^2\right)} \tag{14}$$

Obtain: $\alpha=\dfrac{1}{1+\mu}$

2.4 Solution to the optimal damping ratio

At the highest point of the H and K curves, make $\dfrac{\partial S^2}{\partial\lambda^2}=0$, $\dfrac{h}{k}=\dfrac{1}{\left[1-\lambda^2-\mu\lambda^2\right]^2}$,

Find the optimal damping ratio of the damping ram as: $\xi=\sqrt{\dfrac{3\mu}{8(1+\mu)}}$

3 Parameter Calculation of Damping Ram

Add local contact without penetration to the eight diagonal iron and the contact surface between the iron and the sliding pillow at the upper and lower ends of the tool holder, and add fixed constraints on the back. Apply tangential cutting force at the top of the sliding pillow, and conduct finite element analysis on the maximum elongation of the hollow vibration damping sliding pillow vertically, as shown in Figure 4:

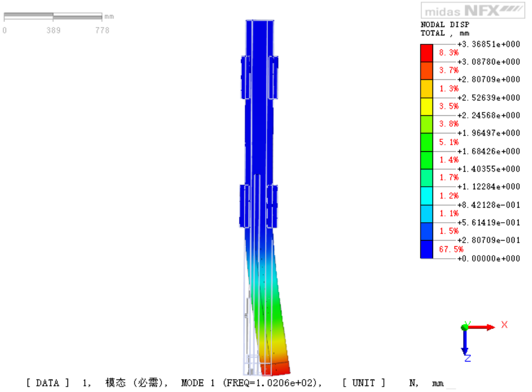

Figure 4 Modal Frequency Response Diagram

In the figure, we can see that the first-order modal resonance frequency of the damping ram is $f = 102.06 Hz$.

3.1 Main parameter calculation

We can calculate the natural vibration angular frequency of the damping ram through first-order modal analysis as follows:

$$\omega_N = 2\pi f = 640.88 \ rad/s \tag{15}$$

Here we use software to calculate the masses M1 and M2 of the ram and damping block: $M_1 = 757.46 \ Kg$ $M_2 = 69.31 \ Kg$

The mass ratio of the damping ram is:

$$\mu = \frac{M_2}{M_1} = \frac{69.31}{757.46} = 0.0915 \tag{16}$$

Natural frequency ratio: $\alpha = \frac{1}{1+\mu} = 0.916$

The homology frequency ω_N is:

$$\omega_n = \alpha \cdot \omega_N = 587.05 \ rad/s \tag{17}$$

The equivalent stiffness K of the shock absorber mirror rod is:

$$K = M\omega_n^2 = 311109.405 \ N/mm \tag{18}$$

The stiffness K of the power absorber is:

$$K = M\omega_n^2 = 23886.8 \ N/mm \tag{19}$$

optimal damping ratio: $\xi = \sqrt{\frac{3\mu}{8(1+\mu)}} = \sqrt{\frac{3\times 0.0915}{8\times 1.0916}} = 0.177$.

The damping of the power absorber can be obtained as:

$$c = 2\xi m\omega_n = 14403.95 N\cdot s/m \tag{19}$$

3.2 Selection of damping fluid

The magnitude of the damping coefficient of the damping fluid depends on the viscosity of the damping fluid, which is calculated using the kinematic viscosity in reference [1] $v = \frac{\mu}{\rho} = \frac{c}{128lp}$.

By searching for literature, it has been found that methyl silicone oil has good damping properties and various physical and chemical properties, which can provide a large damping coefficient. Therefore, methyl silicone oil is used as the damping fluid for the damping ram.

4 Simulation of Vibration Damping Ram

4.1 Establishing a simulation analysis model for damping dynamic vibration damping sleepers

We have chosen the Midas NFX finite element analysis software to analyze the vibration damping ram. In the process of establishing a simulation model of the damping dynamic vibration damping ram, we should try to restore the movement of the ram under real conditions as much as possible. The work of the ram cannot be separated from the precise fit of components such as the slide seat, balance cylinder, and rolling screw.If we model and analyze all components such as the slide seat, balance oil cylinder, and rolling screw when establishing a simulation analysis model for damping dynamic vibration reduction sleepers, it will greatly increase our workload and work difficulty.Therefore, we need to simplify the simulation analysis model of the damping ram while meeting the actual working conditions of the ram.(The slide seat is a fixed inclined iron and a support iron that wrap around the sliding pillow. The use of a balance oil cylinder is to reduce the driving force of the motor, and the ball screw is the driving element, which has a relatively small impact on the sliding pillow when it is at its maximum extended stroke.)The following principles should be followed: ①The stiffness of the damping ram should not be lower than the maximum stiffness required for actual operation; ②The damping fluid between the damping ram and the internal damping system is replaced by linear damping; ③Except for the damping ram and its built-in damping system, all other parts are considered rigid bodies; The overall analysis model of the damping ram is shown in the figure 5:

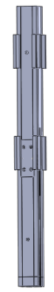

Figure 5 Finite element root system model diagram

4.2 Finite element analysis process of vibration damping ram

4.2.1 Material of damping ram

According to the original VCT16-NC CNC vertical lathe, the material used for turning the tool holder slider is 45 steel. The damping block in the built-in damping system of the slider should be made of materials with higher mass density. Among the metal materials, tungsten has a higher mass density, and the mass density of tungsten alloy can reach 19.3g/cm^3. All its properties meet the working conditions of the damping block. Therefore, tungsten based heavy alloy is chosen as the material with fast damping.

4.2.2 Add constraint

In the simplified model of the tool holder, due to the mutual contact between the damping ram and the slide seat, which is not completely in contact, 16 columns are used as the simplified model of the slide seat. In order to better analyze the damping effect of the slide seat, the simplified model of the slide seat is a rigid body and fixed, and bidirectional sliding is added between the damping ram and the slide seat.As shown in the figure 6:

Figure 6 Analysis Model Constraint Diagram

4.3 Finite element analysis of damping dynamic damping sleeper

In order to visually demonstrate the vibration reduction effect of the damping ram, we used modal analysis method for transient response analysis and conducted comparative experiments between the original tool holder ram and the damping ram. An impact load was applied at the connection of the tool fixture between the original tool holder ram and the damping ram, and the damping ram vibrated after being subjected to the impact load. The vibration amplitude of the two types of rams was observed. In Figure 7, we can visually see the vibration reduction effect of the damping damping ram.

Figure 7 Comparative Test

5 Conclusion

The improvement design of the vertical lathe turning tool holder components analyzed and summarized the problems of machining accuracy and surface smoothness caused by cutting chatter in the processing equipment. A damping dynamic damping ram was designed, and the optimization design and finite element analysis of the damping dynamic damping ram were carried out to minimize the amplitude and frequency of cutting chatter generated during the machining process of the vertical lathe tool holder components.

Fund Projects: ①Science and Technology Research Project of Liaoning Provincial Department of Education：Research on the Application of Damping and Vibration Reduction Technology in Key Components of Machine Tools; (JYTMS20230066) ② The Fund of Liaoning Provincial Natural Science and Technology Foundation Regional Joint（No.2021-YKLH-08).

References

[1]Qin Bai.Study on Dynamic Characteristics Simulation and Optimization Design of Dynamical Vibration Absorption Boring Bar with Damping [J]. Harbin University of Science and Technology, 2009(24):11-19.

[2]Hou Xueyuan, Ren Xueoing, Ren Chong. Structure Design and Dynamic Characteristic Simulation Study of a Vibration Damping Boring Cutter [J]. MACHINE TOOL&HYDRAULICS, 2010(47):21-25.

[3]Yang Liyu.Optimization Design and Simulation Study of Particle Damping and Magnetorheological Composite Damping Boring Cutter [D].North University,2018.

[4]He Miao.Dynamic Characteristics Analysis and Optimization Design of Dynamic Damping Boring Bar [D]. Southeast University For the Academic Degree of Master of Engineering, 2018.

[5]Du Jingxuan. Study on Theory and Experiments for Damping Tools with High Slenderness Ratio [D]. North University, 2013, 4(12):25-29.

[6]Shen Xingquan, Ma teng, Gao Weijia.Research on Flutter Suppressing Device of Deep Hole Machining Based on Magnetorheological Effects [J]. 2017(12):45-19.

[7]Liu Lijia, Liu Xianl. Comprehensive survey of vibration control technology in machining [J]. International Journal of Hybrid Information Technology, 2015, 8(4):307-316.

Publisher: Viser Technology Pte. Ltd.

URL: www.viserdata.com

Add.:21 Woodlands Close, #08-18,

Primz Bizhub SINGAPORE (737854)

ISSN 2661-443X